

Wave function evolution from source to detection and the measurement

Li Hua Yu
Brookhaven National Laboratory

(Dated: 12/17/2024)

We analyze the evolution of a particle wave function when it propagates through free space in the longitudinal z -direction from a thin entrance slit to a detector behind a thin exit slit parallel to the horizontal y -axis. We consider an extra aperture slit between the two slits to probe the evolution of the wave function and close the aperture slit starting from wide open until the detection counting rate in a repeated experiment drops to half. When all the slits are long and thin, the 1D-Schrödinger equation gives the wave function evolution until the final detection. The width of the aperture slit in the vertical x -direction depends on the z -position of the slit providing an approximate description of the wave function evolution. The width of the function characterizing this dependence starts from the entrance slit. It grows wider until it reaches a maximum and then shrinks narrower and finally collapses into the exit slit where the particle is detected. Thus the envelope of this function has a spindle shape with its pointed ends at the two slits. Hence it is very different from the well-known wave function of the Schrödinger equation with the initial condition at the entrance slit, which is narrow only at the beginning, then grows wider until it reaches the exit slit, where it is much larger than the slit width. However, the phase information is lost because the aperture slit distorts the wave function. To keep the phase information, we replace the aperture slit with a thin pin (parallel to the y -axis) that blocks the wave function. We then study its perturbative effect on the counting rate of the detector. This analysis provides a function to probe the process of the wave function collapse right before the detection. We show this function is real-valued, with amplitude and phase information, and is closely related to the wave function.

1. INTRODUCTION

As pointed out by R. Penrose [1][2], “The fundamental problem of quantum mechanics, as that theory is presently understood, is to make sense of the reduction of the state vector (i.e., the collapse of the wavefunction).” “This issue is usually addressed in terms of the quantum measurement problem, which is to comprehend how, upon measurement of a quantum system, this (seemingly) discontinuous process can come about.” According to S. Weinberg [3], in this problem, “the difficulty is not that quantum mechanics is probabilistic...The real difficulty is that it is also deterministic, or more precisely, that it combines a probabilistic interpretation with deterministic dynamics.” “This leaves the task of explaining them by applying the deterministic equation for the evolution of the wavefunction, the Schrödinger equation, to observers and their apparatus.” Bohr offered an interpretation that is independent of a subjective observer, or measurement, or collapse; instead, an “irreversible” or effectively irreversible process causes the decay of quantum coherence which imparts the classical behavior of “observation” or “measurement” [4, 5]. The important question is how are the probabilities converted into an actual, well-defined classical outcome? In quantum mechanics, the measurement problem is the problem of how, or whether, wavefunction collapse occurs [5] in this process. Gerard 't Hooft in his discussion [6, 7] about quantum mechanics, pointed out that “In practice, quantum mechanics merely gives predictions with probabilities attached. This should be considered as a normal and quite acceptable feature of predictions made by science: different possible outcomes with different probabilities. In the world that is familiar to us, we always have such a situation when we make predictions. Thus the question remains: What is the reality described by quantum theories? I claim that we can attribute the fact that our predictions come with probability distributions to the fact that not all relevant data for the predictions are known to us, in particular important features of the initial state.”

In this paper, we propose an experiment to provide information that will help address these questions. In this introduction, we will outline our qualitative analysis of the experiment. Then, in the following sections, we will present the derivation and more detailed results quantitatively.

As illustrated in Figure 1, we analyze the wave function evolution of a particle when it propagates through free space in the longitudinal z -direction from a thin entrance slit 1 to a detector behind a thin exit slit 3 to find the information about whether the wave function collapse occurs at the entrance slit 1 or the exit slit 3. The slits are parallel to the y -axis (perpendicular to the plane of the figure). The x -axis is vertical in the figure. Between the slits, the wave function must follow the Schrödinger equation because the only non-unitary (irreversible) process is at the slits, where the wave function is cut off partly. Only the particles that pass through the slits are selected and detected. When the aperture slit 2 is wide open, the process between slit 1 and 3 must follow the Schrödinger equation, and the probability of a particle found between z_1 and z_3 is a constant and independent of $z \equiv z_2$. The caption for Fig. 1 gives the notations. We always use $x = x_2$ and $z = z_2$ to indicate that x and z are variables.

In section 2 we discuss 1D-Schrödinger equation and the propagation of wave function

For simplicity, we neglect the effect of the particle spin, which could be an electron or photon. When we use numerical examples, we consider photons with wavelengths of $0.5\mu m$. In section 2, we shall show that when the slits are long and thin, under the paraxial approximation, the wave function evolution follows the non-relativistic 1D-Schrödinger equation until the final detection. The variables in the wave function are x and t . Because $z = vt$ where v is the particle velocity, it is linear with t , we take z as time. For a photon, $v = c$ is the light speed. The wave function is independent of y .

To probe the wave function evolution before the final detection, we close the aperture slit 2 starting from wide open until the detection counting rate in a repeated experiment drops to half. The counting rate is proportional to the probability $P_{3b} \equiv \int dx_3 |\psi_{3b}(x_3, z_3)|^2$. As shown in Fig. 1, $\psi_{3b}(x_3, z_3)$ is the probability amplitude of the wave function behind the exit slit 3. P_{3b} is a function of σ_2, s_2 , and z , where the aperture width σ_2 is defined by a Gaussian $f_2(x_2) = \exp(-\frac{1}{4\sigma_2^2}(x_2 - s_2)^2)$, and s_2 is the center position of slit 2. When slit 2 is wide open (i.e., $\sigma_2 \rightarrow \infty$), P_{3b} becomes a constant independent of z and s_2 . We denote it as $P_{3bo} = P_{2b}(\sigma_2 = \sigma_3, s_2 = s_3, z_2 = z_3)$. However, we need to specify how to search σ_2 such that $P_{3b}(\sigma_2, s_2, z) = \frac{1}{2}P_{3bo}$.

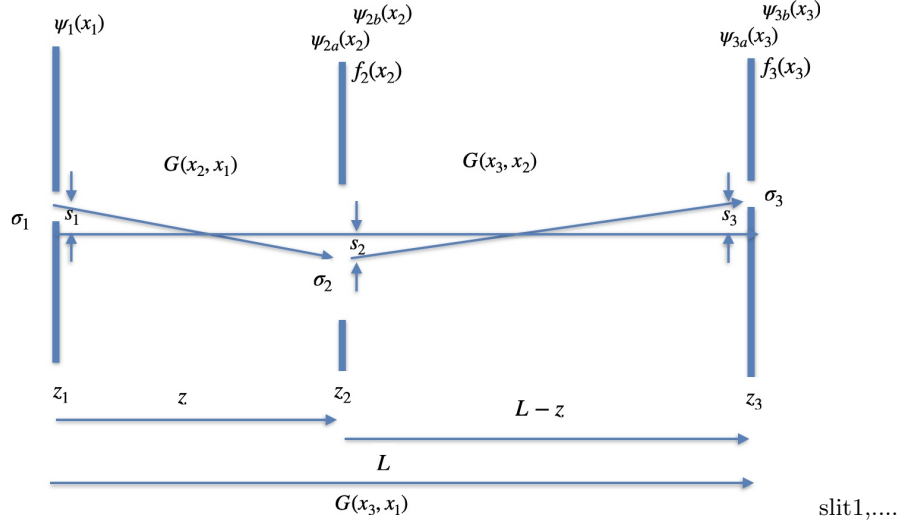


FIG. 1. The wave functions at slits 1,2,3 at z_1, z_2, z_3 with apertures $\sigma_1, \sigma_2, \sigma_3$ and corresponding transverse displacements s_1, s_2, s_3 in x -direction. The distances between the slits are $z, L-z, L$. The longitudinal is the z -axis, vertical is the x -axis. The slits are perpendicular to the plane of the figure, parallel to the y -axis. We use $\psi_1(x_1, z_1), \psi_{2a}(x_2, z_2)$ and $\psi_{2b}(x_2, z_2), \psi_{3a}(x_3, z_3)$ and $\psi_{3b}(x_3, z_3)$ to represent the wave function at the entrance, the middle aperture, and the exit slit, respectively. The subscripts a and b represent before and after the corresponding slits. We use $f_2(x_2)$ and $f_3(x_3)$ to represent the effect of the slits such that $\psi_1(x_1, z_1) \equiv f_1(x_1), \psi_{2b}(x_2, z_2) = f_2(x_2)\psi_{2a}(x_2, z_2), \psi_{3b}(x_3, z_3) = f_3(x_3)\psi_{3a}(x_3, z_3)$. If we choose the slit with the hard-edged opening, $f_2(x_2)$ and $f_3(x_3)$ would be zero outside the slits and equal to 1 within the slits. To simplify the calculation, we assume they are Gaussian with peak value 1, except that we choose $f_1(x_1)$ to normalize ψ_1 as $P_1 = \int dx_1 |\psi_1(x_1, z_1 = 0)|^2 = 1$.

In Section 3 we calculate the centroid $s_{2max}(z)$ and half width function $\sigma_{2HM}(s_{2max}(z))$ generated by the aperture slit 2

When we search for σ_2 such that $P_{3b}(\sigma_2, s_2, z) = \frac{1}{2}P_{3bo}$, we need to scan both s_2 and σ_2 for a given z . For each z and σ_2 , there is a $s_2 = s_{2max}(z)$ where the counting rate $P_{3b}(\sigma_2, s_2, z)$ reaches maximum. For each z , we scan σ_2 and for each σ_2 we always choose $s_2 = s_{2max}(z)$ as the center of slit 2 to calculate $P_{3b}(\sigma_2, s_2 = s_{2max}(z), z)$ until $P_{3b} = \frac{1}{2}P_{3bo}$. The width σ_2 obtained this way depends on z . This width function, which is denoted as $\sigma_{2HM}(s_{2max}(z))$, and the slit 2 centroid $s_{2max}(z)$ provide an approximate description of the wave function evolution between slits 1 and 3. The width $\sigma_{2HM}(s_{2max}(z))$ is narrow from the beginning at the entrance slit. It grows wider until it reaches a maximum and then shrinks narrower and finally collapses into the exit slit where the particle is detected. Thus the envelope of this function has a spindle shape with its pointed ends at the two slits shown in Figure 2. Hence it is very different from the well-known wave function solution $\psi_{2a}(x_2, z)$ of the Schrödinger equation if the slit 2 is wide open: with the initial condition $\psi_{2a}(x_2, z = z_1) = \psi_1(x_1 = x_2, z_1)$ at the entrance slit 1, $\psi_{2a}(x_2, z)$ is only narrow at the beginning, then growing wider until it reaches the exit slit where $\psi_{2a}(x_2, z = z_3)$ is much larger than the width of exit slit 3 (see the blue curve in Fig.2). We compare the function $s_{2max}(z) \pm \sigma_{2HM}(s_{2max}(z))$ for $s_3 = 0, 1mm, 3mm$ with the RMS width of $|\psi_{2a}(x_2, z)|^2$. For this example, the photon wavelength is $\lambda = 0.5\mu m$, and $z_3 = 2m, \sigma_1 = 50\mu m, \sigma_3 = 4\mu m$. From Fig.2 we see that $\sigma_{2HM}(s_{2max}(z))$ and $s_{2max}(z)$ describe specific events for particles detected at various exit slits at $s_3 = 0, 1mm, \dots, 3mm$, while the well-known wave function $\psi_{2a}(x_2, z)$ is the probability amplitude; it describes the probability distribution along the x -axis. The functions $\sigma_{2HM}(s_{2max}(z))$ and $\psi_{2a}(x_2, z)$ have entirely different physical meanings and shapes.

In Section 4 we derive Perturbative function $\frac{\delta}{\delta f_2(x_2)}P_{3b}$ and its integral $\frac{1}{2} \int_{-\infty}^{\infty} dx_2 \frac{\delta}{\delta f_2(x_2, z=z_2)}P_{3b}$ and discuss its physical meaning

However, the phase information is lost during the scanning process to obtain $s_{2max}(z)$ and $\sigma_{2HM}(s_{2max}(z))$ because the aperture distorts the wave function. To reduce the effect of the aperture on the wave function so we can retain the phase information, we replace it with a thin pin of width Δx_2 parallel to the y -axis that blocks the wave function, i.e., the wave function becomes zero after passing through the pin. We then study the perturbative effect of the pin

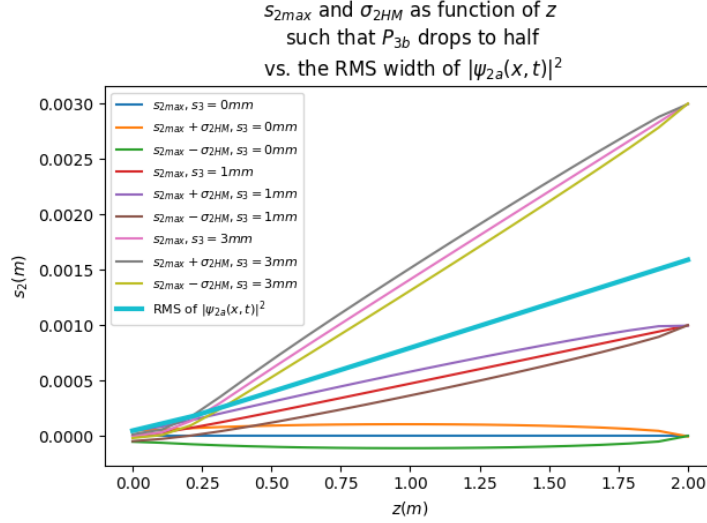


FIG. 2. plot z vs. $\sigma_{2HM}(s_{2max}(z))$ and $s_{2max}(z) \pm \sigma_{2HM}(s_{2max}(z))$ for $s_3 = 0, 1mm, 3mm$ and compare with the RMS width of $|\psi_{2a}(x_2, z = z_1)|^2$, photon wave length $\lambda = 0.5\mu m$, $z_3 = 2m$, $\sigma_1 = 50\mu m$, $\sigma_3 = 4\mu m$.

on the counting rate P_{3b} when Δx_2 is sufficiently small. This analysis generates a function we denote as $\frac{\delta}{\delta f_2(x_2)} P_{3b}$. This function provides information for the wave function evolution process right before the detection. We find that $\frac{\delta}{\delta f_2(x_2)} P_{3b}$ is the functional derivative of detection probability $P_{3b} = \int dx_3 |\psi_3(x_3, z_3)|^2$ with respect to the perturbation of the aperture function $f(x_2)$ at position (x_2, z_2) when it is wide open, i.e. $f(x_2) = 1$. Because of this, during derivation, we also denote $\frac{\delta}{\delta f_2(x_2)} P_{3b}$ as $\frac{\delta}{\delta \chi(x)} P_{3bo}$ with χ representing the pin and P_{3bo} representing the wide-open slit 2. If at a point x_2 , $\frac{\delta}{\delta f_2(x_2)} P_{3b} > 0$, the contribution of Δx_2 is $\Delta P_{3b} = \Delta x_2 \frac{\delta}{\delta f_2(x_2)} P_{3b}$ gives the increase of the counting rate, then the pin decreases the counting rate given by P_{3b} . If $\frac{\delta}{\delta f_2(x_2)} P_{3b} < 0$, the pin blocking at x_2 will increase the counting rate. We show the function is real-valued, with both amplitude and phase information, and is closely related to the wave function and proportional to the product of two Feynman propagators $G(x_3, x_2)G(x_2, x_1)$, i.e., the probability amplitude of the path integral from x_1 passing through x_2 to reach x_3 . Here, $G(x_2, x_1)$ is the Green's function of the Schrödinger equation, the transition probability amplitude from x_1, t_1 to x_2, t_2 , the Feynman propagator.

For the same example in Fig.2, we compare $\frac{\delta}{\delta f_2(x)} P_{3b}$ (green) with $|\psi_{2a}(x)|^2$ (red), and $\text{Re}(\psi_{2a}(x))$ (magenta) in Fig.3, where $s_3 = 3mm$, $z = 1.85m$. The phase of $\frac{\delta}{\delta f_2(x)} P_{3b}$ advances with respect to x very fast when $x < 2mm$ or $x > 4mm$. Its advance rate becomes slow for $2mm < x < 4mm$. It is zero at $x = x_{c0} \approx 2.92mm$ where we use a blue vertical line to mark the point. Because of the fast phase advance, the green curve has a very high oscillation frequency and is hardly visible except near x_{c0} . Near x_{c0} , the phase advance is slow, the oscillation frequency is low, and the fringes are relatively easy to detect in the experiment. We also observe that the oscillation frequency for $\frac{\delta}{\delta f_2(x)} P_{3b}$ in the x direction is much higher than that of $\text{Re}(\psi_{2a}(x))$, and that we do not have a way to measure $\psi_{2a}(x)$ but $\frac{\delta}{\delta f_2(x_2)} P_{3b}$ can be measured, as to be discussed in section 5.

Our calculation shows that $\frac{1}{2} \int_{-\infty}^{\infty} dx_2 \frac{\delta}{\delta f_2(x_2)} P_{3b} = P_{3b}$ is independent of z , i.e. the longitudinal position of the perturbative probe pin. For the example in Fig.3, $P_{3b} = 0.0004258$. It is just half the area between the green curve and the x -axis. The dominating contribution to the area comes from the area near x_{c0} . Far from x_{c0} , the positive and negative parts of the green curve cancel each other, so their contribution to the probability is negligible. Similarly, because of probability conservation, $P_{2a} = \int dx |\psi_{2a}(x, z)|^2 = 1$ is also independent of z .

Thus, once the experiment agrees with the prediction from $\frac{\delta}{\delta f_2(x_2, z=z_2)} P_{3b}$, anywhere between slit 1 and 3, even for $z_2 = z = 0_+$ right after the beginning, the total probability is already determined as $P_{3b} = \frac{1}{2} \int_{-\infty}^{\infty} dx_2 \frac{\delta}{\delta f_2(x_2, z=z_2)} P_{3b}$, i.e., the final detection probability. When slit 2 is wide open, the ‘‘irreversible process,’’ as a non-unitary process, can only occur at either slit 1 or 3. $P_1 = 1$ at the entrance slit 1, and it immediately jumps to $P_{3b} = 0.0004258$ at $z_2 = z = 0_+$, hence the probability collapses at slit 1. Thus, we can divide the process into two parts: (1). The

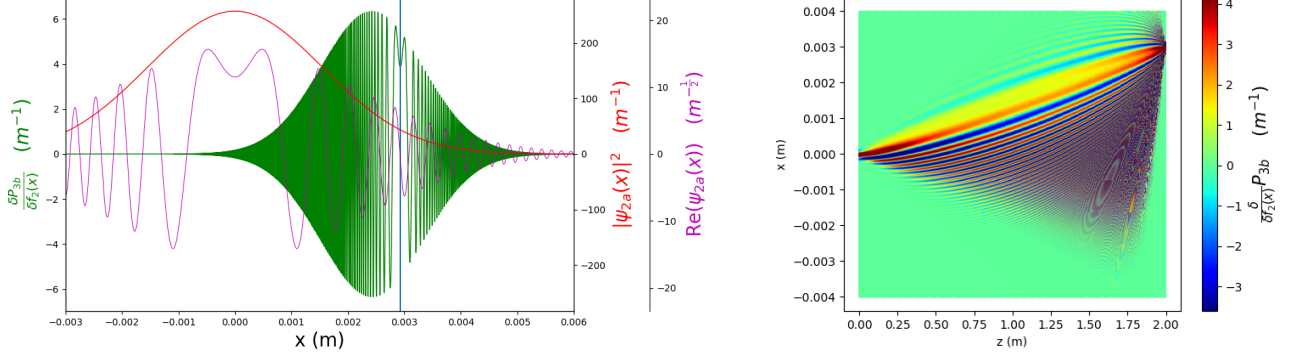


FIG. 3. (a) Compare the function $\frac{\delta P_{3b}}{\delta f_2(x)}$ with $|\psi_{2a}(q_2, t_1)|^2$ (red), and $\text{Re}(\psi_{2a}(x))$ (magenta), $s_3=3mm$, $z = 1.95m$. (b) $\frac{\delta P_{3b}}{\delta f_2(x)}$ vs. x, z in color scale

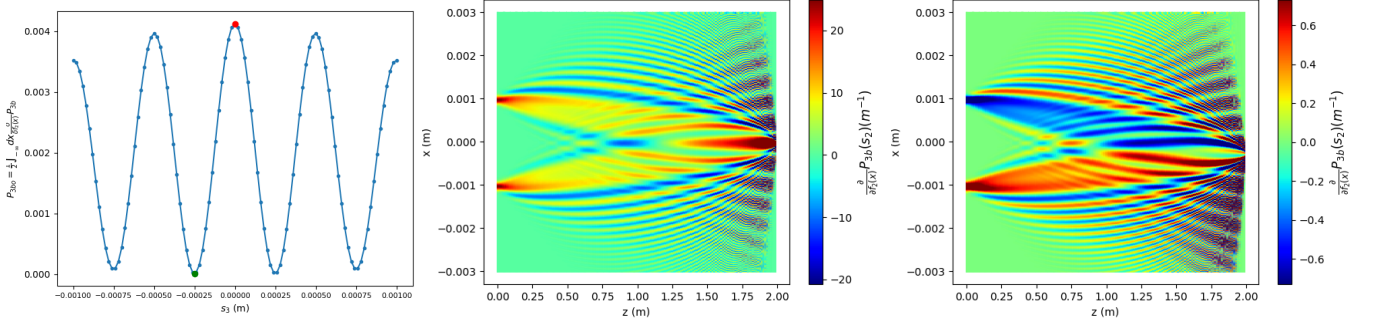


FIG. 4. (a) Interference pattern of $P_{3b}(s_3)$ at $z_3 = 2m$ detector, for $\lambda = 0.5\mu m$. (b) $\frac{\delta}{\delta f_2(x)} P_{3b}(s_2)$ vs. z, x , at maximum $P_{3b} = 0.004122$ at $s_3 = 0$. (c) $\frac{\delta}{\delta f_2(x)} P_{3b}(s_2)$ at minimum $s_3 = -0.25mm$ $P_{3b} = 1.249 \times 10^{-5}$

conceptual wave function collapses, or, in other words, the probability distribution from total probability 1 collapses to one specific individual event with the probability $P_{3b} = 0.0004258$, i.e., one specific case (i.e., the detection by the detector at 3 mm) from a statistical distribution is selected; (2). The continuous physical evolution process: from the start, $\frac{\delta}{\delta f_2(x_2)} P_{3b}$ grows wider and then becomes narrower until it finally collapses into the exit slit. If the exit slit is sufficiently narrow, we take this as the wave packet collapses into a point. This process appears closely related to the discussion of t' Hooft [7] we mention at the beginning.

In Section 5 we describe wave packet propagation in an interference experiment

To demonstrate the phase information inherent in $\frac{\delta}{\delta f_2(x_2)} P_{3b}$, we study an interference experiment as shown in Fig. 4. We replace the single entrance slit 1 in Fig.1 by two slits with $\psi_1(x_1) = \frac{(\psi_{1+}(x_1) + \psi_{1-}(x_1))}{\sqrt{2}}$, where $\psi_{1+}(x_1), \psi_{1-}(x_1)$ are Gaussian with the same width σ_1 but centered at $s_1 = 1mm$ and $s_1 = -1mm$ respectively, and they are in phase. Their separation $2s_1 \gg \sigma_1$, so their overlap is negligible, and hence the normalization $P_1 = \int dx_1 |\psi_1(x_1, z_1 = 0)|^2 = 1$ is satisfied. The other parameters are the same as in Fig. 2. Fig. 4(a) shows $P_{3b}(s_3) = \frac{1}{2} \int_{-\infty}^{\infty} dx_2 \frac{\delta}{\delta f_2(x_2, z=z_2)} P_{3b}$ calculated at $z = 1.9m$. However, as discussed above, the plot is independent of z : it is the same for any $0 < z < 2m$. In Fig. 4(b), when we choose $s_3 = 0$, shown as the red dot in Fig. 4(a), where $P_{3b} = 0.004122$ reaches the peak, there are two spindle-shaped regions symmetrically oriented where $\frac{\delta}{\delta f_2(x_2)} P_{3b} > 0$ varies slowly, and both colored as between yellow to deep red, the two regions are in phase. In Fig.4(c), we choose $s_3 = -0.25mm$, shown as the green dot in Fig. 4(b), where $P_{3b} = 1.249 \times 10^{-5}$ reaches the minimum; the two spindle-shaped regions have different colors. In the upper plane, the region is colored blue. The lower region is colored red, with phases differing by π .

Outline of the more detailed derivation and calculation in sections 2-6

In Section 2, we show that the wave function evolution discussed in Fig. 1 follows the non-relativistic 1D-Schrödinger equation under the paraxial approximation until the final detection. We apply the Green's function of the 1D-Schrödinger equation in steps to find the expressions of $\psi_{2a}, \psi_{2b}, \psi_{3a}, \psi_{3b}$ from the initial wave function ψ_1 .

Then in Section 3 we use the wave function derived in Section 2 to calculate P_{3b} as a function of s_2, σ_2 and $z_2 \equiv z$. This then leads to $s_{2max}(z)$ and the corresponding width function $\sigma_{2HM}(s_{2max}(z))$ discussed above in Section 1.2 and shown in Fig.2, where the spindle-shaped function gives an approximate description of the wave function evolution between slits 1 and 2.

In Section 4, we show that the perturbative probe pin scan generates the functional derivative of P_{3b} , i.e. $\frac{\delta}{\delta f_2(x_2)} P_{3b}$. Then we derive the analytical expression for P_{3b} and $\frac{\delta}{\delta f_2(x_2)} P_{3b}$ by applying the expression of wave functions derived in Section 2. In the derivation, we show that $\frac{1}{2} \int_{-\infty}^{\infty} dx_2 \frac{\delta}{\delta f_2(x_2)} P_{3b} = P_{3b}$ is independent of z_2 , and $\frac{\delta}{\delta f_2(x_2)} P_{3b}$ is proportional to the product of the Green's function $G(x_3, x_2)G(x_2, x_1)$ when the width σ_1 and σ_2 both approach zero, i.e., the probability amplitude from x_1 passing through x_2 to x_3 . We show that when σ_1, σ_3 approach zero, and when slit 2 is wide open, the limit of P_{3b} has a very simple expression. From the expression of $\frac{\delta}{\delta f_2(x_2)} P_{3b}$ we derived its width as a function of z . One can use these expressions to check with the experiment. Then we estimate the required counting number to achieve a specified precision of $\frac{\delta}{\delta f_2(x_2)} P_{3b}$ in the experiment.

In Section 5, we briefly outline the calculation of the interference patterns in Fig. 4 to show the importance of the phase information provided by the function $\frac{\delta}{\delta f_2(x_2)} P_{3b}$.

Section 6 is the summary.

2. 1D-SCHRÖDINGER EQUATION AND THE PROPAGATION OF WAVE FUNCTION

2.1. Paraxial approximation of 2D-Schrödinger equation and Maxwell equation

We first study the wave function evolution between the slits in Fig. 1. Between slits the wave function $\phi(x, z, t)$ must follow the Schrödinger equation,

$$i\hbar \frac{\partial}{\partial t} \phi(x, z, t) = \left(\frac{P_x^2}{2M} + \frac{P_z^2}{2M} \right) \phi(x, z, t) = \left(-\frac{\hbar^2}{2M} \frac{\partial^2}{\partial x^2} - \frac{\hbar^2}{2M} \frac{\partial^2}{\partial z^2} \right) \phi(x, z, t) \quad (1)$$

We do not include y in the variables of the wave function because we consider the system to be independent from y . P_x, P_z are the momentum operators.

Under the paraxial approximation (see e.g., [8–10]), we assume it can be approximated as a plane wave propagating in the z -direction such that we can write it in the form $\phi(x, z, t) = \exp(i(kx - \omega_k t)) \psi(x, z)$, where $\exp(i(kx - \omega_k t))$ with particle energy $E_k = \hbar\omega_k = \frac{\hbar^2 k^2}{2M}$ and momentum $p_z = \hbar k$ represents the plane wave, $kx - \omega_k t$ is its fast-varying phase, and $\psi(x, z)$ is its factor of slowly varying amplitude and phase, so $\psi(x, z)$ represents the deviation from the plane wave. Under the condition for this approximation $|k^2 \psi| \gg |\frac{\partial^2 \psi}{\partial z^2}|$, $|2k \frac{\partial \psi}{\partial z}| \gg |\frac{\partial^2 \psi}{\partial z^2}|$, we have $P_z^2 \phi = \hbar^2 e^{i(kz - \omega_k t)} \left(k^2 - 2ik \frac{\partial}{\partial z} - \frac{\partial^2}{\partial z^2} \right) \psi$, i.e. we can ignore the terms $-\frac{\partial^2 \psi}{\partial z^2}$ compared with $k^2 \psi - 2ik \frac{\partial \psi}{\partial z}$.

$$\begin{aligned}
\frac{P_z^2}{2M}\phi &= \frac{\hbar^2}{2M}e^{i(kz-\omega_k t)}\left(k^2 - 2ik\frac{\partial}{\partial z} - \frac{\partial^2}{\partial z^2}\right)\psi \approx \frac{\hbar^2}{2M}e^{i(kz-\omega_k t)}\left(k^2 - 2ik\frac{\partial}{\partial z}\right)\psi \\
i\hbar\frac{\partial}{\partial t}\phi(x, z, t) &= e^{i(kz-\omega_k t)}\hbar\omega_k\psi = e^{i(kz-\omega_k t)}\frac{\hbar^2 k^2}{2M}\psi \\
\left(\frac{P_x^2}{2M} + \frac{P_z^2}{2M}\right)\phi(x, z, t) &= e^{i(kz-\omega_k t)}\left(\frac{P_x^2}{2M} + \frac{\hbar^2 k^2}{2M} - \frac{ik\hbar^2}{M}\frac{\partial}{\partial z}\right)\psi
\end{aligned} \tag{2}$$

Substituting into Eq.(1), and using $v = \frac{\hbar k}{M}$ as the velocity of the particle with momentum $p_z = \hbar k = Mv$, we get the 1D-Schrödinger equation,

$$i\hbar v\frac{\partial}{\partial z}\psi = -\frac{\hbar^2}{2M}\frac{\partial^2}{\partial z^2}\psi \tag{3}$$

When we consider z taking the role of time with $z = vt$, we get the more familiar form of the 1D-Schrödinger equation,

$$i\hbar\frac{\partial}{\partial t}\psi = -\frac{\hbar^2}{2M}\frac{\partial^2}{\partial x^2}\psi \tag{4}$$

We may rewrite the Eq.(3) as $i\frac{\partial}{\partial z}\psi = \left(-\frac{\hbar}{2Mv}\frac{\partial^2}{\partial x^2}\right)\psi = -\frac{1}{2k}\frac{\partial^2}{\partial x^2}\psi$, then the only parameter in the experiment we discussed in Fig. 1 is $k = \frac{2\pi}{\lambda}$. To calculate all the functions listed in Fig. 1: $\psi_{2a}, \psi_{2b}, \psi_{3a}, \psi_{3b}$ we only need to specify the de Broglie wavelength $\lambda = 0.5\mu\text{m}$ in addition to the specification of the slits ($z_j \equiv vt_j, s_j, \sigma_j; j = 1, 2, 3$) to specify the experiment, all in units of length. So the result can be expressed by a combination of lengths and some dimensionless parameters of the ratio of lengths. This helps to guide us to find simpler expressions.

Similarly, we assume a 2D Maxwell equation (because we do not consider polarization, we just use ϕ to denote any component of the electromagnetic field),

$$\frac{1}{c^2}\frac{\partial^2}{\partial t^2}\phi(x, z, t) = \left(\frac{\partial^2}{\partial x^2} + \frac{\partial^2}{\partial z^2}\right)\phi(x, z, t) \tag{5}$$

Following the same way [9], we assume $k = \frac{\omega}{c}$, $\phi(x, z, t) = e^{i(kz-\omega t)}\psi(x, z)$, take the paraxial approximation: $|\frac{\partial^2}{\partial z^2}\psi| \ll |\frac{\partial^2}{\partial x^2}\psi|$, $|\frac{\partial^2}{\partial z^2}\psi| \ll 2k|\frac{\partial}{\partial z}\psi|$, we get the same equation $i\frac{\partial}{\partial z}\psi = -\frac{1}{2k}\frac{\partial^2}{\partial x^2}\psi$. Then, let $v = c$, $z = vt$, $p_z = k\hbar = Mv$, it is the same as Eq.(4) again. Again, we still can characterize the experiment by specifying $\lambda = \frac{2\pi}{k}$ only.

2.2 Green's function and the propagation of wave function

The Green's function of free space 1D-Schrödinger equation Eq.(4) is in basic quantum physics [11],

$$G(x_2, x_1; t_2 - t_1) = \left(\frac{M}{2\pi i\hbar(t_2 - t_1)}\right)^{\frac{1}{2}} \exp\left[i\frac{M}{2\hbar(t_2 - t_1)}(x_2 - x_1)^2\right] \tag{6}$$

We write another derivation of the Green's function in the Heisenberg picture [12] in Appendix I because later in the Summary section 6, we shall use the derivation process to explain why the position of the detector at the exit slit can affect at the entrance slit the initial wave packet that will evolve into the exit slit at the end.

The initial wave function at slit 1 is $\psi_1(x_1) = f_1(x_1) = \left(\frac{1}{2\pi\sigma_1^2}\right)^{\frac{1}{4}} \exp\left(-\frac{1}{4\sigma_1^2}(x_1 - s_1)^2\right)$, normalized with $P_1 = \int dx_1 |\psi_1(x_1, z_1)|^2 = 1$. For the wave function propagation from slit 1 to 3, we first calculate the wave function $\psi_{2a}(x_2, t_2) = \int dx_1 G(x_2, x_1; t_2 - t_1) \psi_1(x_1)$. After passing through the slit 2, we have $\psi_{2b}(x_2, z_2) = f_2(x_2) \psi_{2a}(x_2, z_2)$. This propagation continues to slit 3 as $\psi_{3a}(x_3, z_3)$ and $\psi_{3b}(x_3, z_3)$, so we have

$$\begin{aligned}\psi_{2a}(x_2, z_2) &= \int dx_1 G(x_2, x_1; t_2 - t_1) \psi_1(x_1, z_1) \\ \psi_{2b}(x_2, z_2) &= f_2(x_2) \psi_{2a}(x_2, z_2) \\ \psi_{3a}(x_3, z_3) &= \int dx_2 G(x_3, x_2; t_3 - t_2) \psi_{2b}(x_2, z_2) \\ \psi_{3b}(x_3, z_3) &= f_3(x_3) \psi_{3a}(x_3, z_3)\end{aligned}\tag{7}$$

For the first step of propagation, because both $\ln \psi_1(x_1, z_1)$ and $\ln G(x_2, x_1; t_2 - t_1)$ are quadratic forms of x_1 , this is a Gaussian integral. Use the notations of section 2.1: $z_j \equiv vt_j$, $\frac{Mv}{\hbar} = k = \frac{2\pi}{\lambda}$ and $z = z_2 - z_1 = v(t_2 - t_1)$ in Fig. 1, we have

$$\begin{aligned}\ln \psi_1(x_1, z_1 = 0) &= \alpha_1(x_1 - s_1)^2 + c_1 \\ \alpha_1 &= -\frac{1}{4\sigma_1^2}, c_1 = \frac{1}{4} \ln \left(\frac{1}{2\pi\sigma_1^2} \right) \\ \ln G(x_2, x_1; t_2 - t_1) &= i\beta_1(x_2 - x_1)^2 + \frac{1}{2} \ln \frac{\beta_1}{i\pi} \\ \beta_1 &= \frac{M}{2\hbar(t_2 - t_1)} \equiv \frac{1}{4d_1}, d_1 = \frac{\hbar t}{2M} = \frac{z}{2k} = \frac{\lambda z}{4\pi} \\ \psi_{2a}(x_2, z_2) &= \int dx_1 \exp(\alpha_1(x_1 - s_1)^2 + i\beta_1(x_2 - x_1)^2 + c_1 + \frac{1}{2} \ln \frac{\beta_1}{i\pi})\end{aligned}\tag{8}$$

The exponent of the integrand in $\psi_{2a}(x_2, z_2)$ can be written into a standard quadratic form of $ax_1^2 + bx_1 + c$. It is then integrated out using the following Gaussian integral, which is to be applied repeatedly in the next steps, as long as the real part of a is negative.

$$\int dx \exp(ax^2 + bx + c) = \left(\frac{\pi}{-a}\right)^{\frac{1}{2}} \exp\left(-\frac{b^2}{4a} + c\right) = \exp\left(-\frac{b^2}{4a} + c + \ln\left(\frac{\pi}{-a}\right)^{\frac{1}{2}}\right),\tag{9}$$

In the following applications of this formula, we always checked that indeed $\text{Re}(a) < 0$. The result is written into the same standard quadratic form as $\ln \psi_1(x_1, z_1)$, but in terms of the variable x_2

$$\begin{aligned}\ln \psi_{2a}(x_2, t) &= \alpha_{2a}(x_2 - s_{2a})^2 + c_{2a} \\ \alpha_{2a} &= \frac{i\alpha_1\beta_1}{(\alpha_1 + i\beta_1)} = \frac{1}{\frac{1}{\alpha_1} + \frac{1}{i\beta_1}} = -\frac{1}{4\sigma_1^2 + id_1} \equiv -\frac{1}{4\Delta_1} \\ s_{2a} &= s_1 \\ c_{2a} &= \frac{1}{2} \ln \left(\frac{\alpha_{2a}}{\alpha_1} \right) + c_1 = \frac{1}{2} \ln \left(\frac{\sigma_1^2}{\sigma_1^2 + id_1} \right) + \frac{1}{4} \ln \left(\frac{1}{2\pi\sigma_1^2} \right)\end{aligned}\tag{10}$$

Here we defined a parameter $\Delta_1 \equiv \sigma_1^2 + id_1$ so that $\alpha_{2a} = -\frac{1}{4\Delta_1}$ is similar to $\alpha_1 = -\frac{1}{4\sigma_1^2}$, with the width σ_1^2 replaced by Δ_1 .

The next step is to pass through the slit 2 with $f_2(x_2) = \exp(\alpha_{f2}(q_2 - s_2)^2)$, $\alpha_{f2} \equiv -\frac{1}{4\sigma_2^2}$, the result of applying $\psi(x_2) = f_2(x_2)\psi_{2a}(x_2)$ is

$$\begin{aligned} \ln \psi_{2b}(x_2, z_2 = z) &= \alpha_{2b}(x_2 - s_{2b})^2 + c_{2b} \\ \alpha_{2b} &= \alpha_{2a} + \alpha_{f2} \\ s_{2b} &= \frac{\alpha_{2a}s_{2a} + \alpha_{f2}s_2}{\alpha_{2a} + \alpha_{f2}} \\ c_{2b} &= -\alpha_{2b}s_{2b}^2 + \alpha_{2a}s_{2a}^2 + \alpha_{f2}s_2^2 + c_{2a} \end{aligned} \quad (11)$$

The next two steps in Eq.(7) to pass from slit 2 to slit 3 and calculate $\psi_{3a}(x_3), \psi_{3b}(x_3)$ are almost a repetition of the calculation of $\psi_{3a}(x_3), \psi_{3b}(x_3)$ in Eq.(10) and Eq.(11), except that in this wave function propagation calculation from slit 2 to before slit 3, the Green's function is different from Eq.(8) with replaced variables x_2, x_3, β_2, d_2 ,

$$\begin{aligned} \ln G(x_3, x_2; t_3 - t_2) &= i\beta_2(x_3 - x_2)^2 + \frac{1}{2} \ln \frac{\beta_2}{i\pi} \\ \beta_2 &= \frac{M}{2\hbar(t_3 - t_2)} = \frac{k}{2(L - z)} \equiv \frac{1}{4d_2}, d_2 = \frac{L - z}{2k} = \frac{\lambda(L - z)}{4\pi} \\ f_3(x_3) &= \exp\left(-\frac{1}{4\sigma_3^2}(x_3 - s_3)^2\right) \equiv \exp(\alpha_{f3}(x_3 - s_3)^2) \end{aligned} \quad (12)$$

In the derivation, we need to introduce another parameter, $\Delta_2 \equiv \sigma_2^2 \frac{\Delta_1}{\Delta_1 + \sigma_2^2} + id_2$ in addition to Δ_1 . This helps us to find a pattern in the repetitive steps as given in the Appendix II. The result is

$$\begin{aligned} \ln \psi_1(x_1, z_1) &= \alpha_1(x_1 - s_1)^2 + c_1 = -\frac{1}{4\sigma_1^2}(x_1 - s_1)^2 + \frac{1}{4} \ln \left(\frac{1}{2\pi\sigma_1^2} \right) \\ \ln \psi_{2a}(x_2, z_2) &= \alpha_{2a}(x_2 - s_1)^2 + c_{2a} = -\frac{1}{4\Delta_1}(x_2 - s_1)^2 + \frac{1}{2} \ln \left(\frac{\sigma_1^2}{\Delta_1} \right) + \frac{1}{4} \ln \left(\frac{1}{2\pi\sigma_1^2} \right) \\ \ln \psi_{2b}(x_2, z_2) &= \alpha_{2b}(x_2 - s_{2b})^2 + c_{2b} = -\frac{1}{4\Delta_1} \frac{\Delta_1 + \sigma_2^2}{\sigma_2^2} (x_2 - s_{2b})^2 - \frac{(s_1 - s_2)^2}{4(\Delta_1 + \sigma_2^2)} + \frac{1}{2} \ln \left(\frac{\sigma_1^2}{\Delta_1} \right) + \frac{1}{4} \ln \left(\frac{1}{2\pi\sigma_1^2} \right) \\ \ln \psi_{3a}(x_3, z_3) &= \alpha_{3a}(x_3 - s_{3a})^2 + c_{3a} = -\frac{1}{4\Delta_2}(x_3 - s_{2b})^2 - \frac{(s_1 - s_2)^2}{4(\Delta_1 + \sigma_2^2)} + \frac{1}{2} \ln \left(\frac{\sigma_2^2}{\Delta_1 + \sigma_2^2} \frac{\sigma_1^2}{\Delta_2} \right) + \frac{1}{4} \ln \left(\frac{1}{2\pi\sigma_1^2} \right) \\ \ln \psi_{3b}(x_3, z_3) &= \alpha_{3b}(x_3 - s_{3b})^2 + c_{3b} \\ &= -\frac{1}{4\Delta_2} \frac{\Delta_2 + \sigma_3^2}{\sigma_3^2} (x_3 - s_{3b})^2 - \frac{(s_3 - s_{2b})^2}{4(\Delta_2 + \sigma_3^2)} - \frac{(s_1 - s_2)^2}{4(\Delta_1 + \sigma_2^2)} + \frac{1}{2} \ln \left(\frac{\sigma_2^2}{\Delta_1 + \sigma_2^2} \frac{\sigma_1^2}{\Delta_2} \right) + \frac{1}{4} \ln \left(\frac{1}{2\pi\sigma_1^2} \right) \\ s_{2b} &= (s_2 - s_1) \frac{\Delta_1}{\Delta_1 + \sigma_2^2} + s_1 \\ s_{3b} &= (s_3 - s_{2b}) \frac{\Delta_2}{\Delta_2 + \sigma_3^2} + s_{2b} \\ \Delta_1 &\equiv \sigma_1^2 + id_1, \beta_1 = \frac{1}{4d_1}, d_1 = \frac{\lambda z}{4\pi} \\ \Delta_2 &\equiv \sigma_2^2 \frac{\Delta_1}{\Delta_1 + \sigma_2^2} + id_2, \beta_2 = \frac{1}{4d_2}, d_2 = \frac{\lambda(L - z)}{4\pi} = d_L - d_1, d_L \equiv \frac{\lambda L}{4\pi} \end{aligned} \quad (13)$$

with

$$\begin{aligned}
\frac{1}{\alpha_1} &= -4\sigma_1^2 \\
\frac{1}{\alpha_{2a}} &= -4\Delta_1 \\
\frac{1}{\alpha_{2b}} &= -4\sigma_2^2 \frac{\Delta_1}{\Delta_1 + \sigma_2^2} \\
\frac{1}{\alpha_{3a}} &= -4\Delta_2 \\
\frac{1}{\alpha_{3b}} &= -4\sigma_3^2 \frac{\Delta_2}{\Delta_2 + \sigma_3^2}
\end{aligned} \tag{14}$$

To check this result, when using a specific example so that all the coefficients of the quadratic forms in the intermediate steps are numerical, the numerical check of the result using Eq.(7) by Gaussian integration is straightforward and simple.

3. THE PEAK AND WIDTH OF THE WAVE FUNCTION EVOLUTION BETWEEN SLIT 1 AND 3

We use the results from Section 2 to study the wave function evolution between slits 1 and 3, calculate its transverse peak position $s_{2max}(z)$ and the corresponding width function $\sigma_{2HM}(s_{2max}(z))$ introduced in the introduction 1.2 and in Fig. 2. These two functions reflect the effect of slit 2 aperture on the detection probability $P_{3b}(s_2, \sigma_2, z)$ after slit 3. Its dependence on s_2, σ_2 as a function of z provides an approximate description of the wave function evolution as the spindle-shaped region in Fig. 2.

3.1 Probability P_{2b}, P_{3b}

The expression of $\ln \psi_{2b}(x_2, z_2)$ in Eq.(13) is again a quadratic form of x_2 , hence $\ln \psi_{2b}(x_2, z_2) + \ln \psi_{2b}^*(x_2, z_2)$ in the integrand of $P_{2b} = \int dq_2 |\psi_{2b}(x_2)|^2$ is also a quadratic form. Thus Eq.(9) can be applied as a Gaussian integral to get, as derived in Appendix III,

$$\begin{aligned}
P_{2b} &= \int dq_2 |\psi_{2b}(x_2)|^2 = \int dx_2 \exp \left(2\text{Re}(\alpha_{2b})x_2^2 - 2\frac{|\alpha_{2b}|^2 (\text{Im}(s_{2b}))^2}{\text{Re}(\alpha_{2b})} + 2\text{Re}(c_{2b}) \right) \\
P_{2b}(s_2, \sigma_2, z_2) &= \sqrt{\frac{\pi}{-2\text{Re}(\alpha_{2b})}} \exp \left(-2\frac{|\alpha_{2b}|^2 (\text{Im}(s_{2b}))^2}{\text{Re}(\alpha_{2b})} + 2\text{Re}(c_{2b}) \right) \\
P_{3b}(s_3, \sigma_3, z_3) &= \sqrt{\frac{\pi}{-2\text{Re}(\alpha_{3b})}} \exp \left(-2\frac{|\alpha_{3b}|^2 (\text{Im}(s_{3b}))^2}{\text{Re}(\alpha_{3b})} + 2\text{Re}(c_{3b}) \right)
\end{aligned} \tag{15}$$

$P_{3b}(s_3, \sigma_3, z_3)$ is derived just by replacing the subscripts correspondingly.

Substituting the expressions $\alpha_{2b}, s_{2b}, c_{2b}$, etc. in Eq.(13,14) into Eq.(15), as derived in Appendix III, we find P_{2b} expressed in terms of the scaled dimensionless parameters μ, ρ defined in the following,

$$P_{2b} = \sqrt{\frac{\rho\mu^2}{\mu^2 + \rho\mu^2 + 1}} \exp\left(-\frac{1}{2\sigma_1^2} \frac{\mu^2}{\mu^2 + \rho\mu^2 + 1} (s_1 - s_2)^2\right) \quad (16)$$

$$\mu \equiv \frac{\sigma_1^2}{d_1} = \frac{4\pi\sigma_1^2}{\lambda L}, \rho \equiv \frac{\sigma_2^2}{\sigma_1^2}$$

In the limit of small slit sizes, as $\sigma_1, \sigma_2 \rightarrow 0$, we need to specify their ratio $\rho = \frac{\sigma_2^2}{\sigma_1^2}$, we find

$$P_{2b} = \sqrt{\rho\mu^2} \exp\left(-\frac{\mu^2}{2\sigma_1^2} (s_1 - s_2)^2\right) = \frac{\sigma_1\sigma_2}{d_1} \exp\left(-\frac{\sigma_1^2}{2d_1^2} (s_1 - s_2)^2\right) \quad (17)$$

3.2 Peak position $s_{2max}(z)$ and the width function $\sigma_{2HM}(s_{2max}(z))$ compared with $|\psi_{2a}(x_2, z)|^2$

We write $P_{3b}(s_2, \sigma_2, z)$ to explicitly show it is a function of s_2, σ_2 for a given z . We first notice that the exponent $-2\frac{|\alpha_{3b}|^2 (\text{Im}(s_{3b}))^2}{\text{Re}(\alpha_{3b})} + 2\text{Re}(c_{3b})$ in P_{3b} is a quadratic function of s_2 and hence the peak position can be determined by its derivative with respect to s_2 , as is shown in the following.

The only dependence of the term $-2\frac{|\alpha_{3b}|^2 (\text{Im}(s_{3b}))^2}{\text{Re}(\alpha_{3b})}$ is in $(\text{Im}(s_{3b}))^2$ with $s_{3b} = (s_3 - s_{2b})\frac{\Delta_2}{\Delta_2 + \sigma_3^2} + s_{2b}$, and $s_{2b} = (s_2 - s_1)\frac{\Delta_1}{\Delta_1 + \sigma_2^2} + s_1$ in Eq.(13). Thus $\text{Im}(s_{3b})$ is linear in s_2 , i.e. $(\text{Im}(s_{3b}))^2$ is a quadratic form of s_2 , while $\frac{1}{\alpha_{3b}} = -4\sigma_3^2\frac{\Delta_2}{\Delta_2 + \sigma_3^2}$ in Eq.(14) is independent of s_2 , hence $-2\frac{|\alpha_{3b}|^2 (\text{Im}(s_{3b}))^2}{\text{Re}(\alpha_{3b})}$ is a quadratic form of s_2 .

The only dependence of c_{3b} on s_2 is in its two terms $-\frac{(s_3 - s_{2b})^2}{4(\Delta_2 + \sigma_3^2)} - \frac{(s_1 - s_2)^2}{4(\Delta_1 + \sigma_2^2)}$. Thus, $\ln P_{3b}(s_2, \sigma_2, z)$ is also a quadratic form, and $\frac{\partial}{\partial s_2} \ln P_{3b}(s_2, \sigma_2, z) = 0$ is a linear equation easily solved to give $s_{2max}(z, \sigma_2)$, it is a function of z and σ_2 .

About whether $s_{2max}(z)$ always gives a peak, notice that when $|s_2| \rightarrow \infty$, $\ln \psi_{2a}(x_2, z_2) = \alpha_{2a}(x_2 - s_{2b})^2 + c_{2b} \rightarrow -\infty$ because the real part of α_{2b} is always negative, and because $s_{2b} = (s_2 - s_1)\frac{\Delta_1}{\Delta_1 + \sigma_2^2} + s_1$, $|s_2| \rightarrow \infty$ leads to $|s_{2b}| \rightarrow \infty$, the probability of passing through the system approaches zero as $|s_2| \rightarrow \infty$. Hence, $s_{2max}(z)$ is always a peak, as shown in the numerical examples in Figure 5(a).

We substitute $s_{2max}(z, \sigma_2)$ into Eq.(15) and calculate $P_{3b}(\sigma_2, s_2 = s_{2max}(z, \sigma_2))$ as a function of σ_2 for a given $z_2 = z$. This is plotted in Figure 5(b) for a specific example and various z . Notice that when $\sigma_2 \rightarrow \infty$, all the curves for different z approach the same P_{3b} . This is the P_{3b} when there is no aperture slit 2, so Figure 1 shows it should be the same as P_{2b} if we replace slit 3 with slit 2 and set $s_2 \rightarrow s_3, \sigma_2 \rightarrow \sigma_3, z_2 \rightarrow z_3 = L$. We denote this as $P_{3bo} \equiv P_{3b}(s_3, \sigma_3, z_3; \sigma_2 \rightarrow \infty) = P_{2b}(s_2 \rightarrow s_3, \sigma_2 \rightarrow \sigma_3, z_2 \rightarrow z_3)$ to indicate it is at the maximum opening of slit 2.

For the example $\sigma_1 = 50\mu m, \sigma_3 = 4\mu m, s_1 = 0, s_3 = 3mm$, for $z_3 = L = 2m, d_1 = d_L = \frac{\lambda z}{4\pi} = \frac{0.5\mu m \times 2m}{4\pi} = 7.96 \times 10^{-8}$, and $\mu^2 = \left(\frac{\sigma_1^2}{d_1}\right)^2 = \left(\frac{2500 \times 10^{-12}}{7.96 \times 10^{-8}}\right)^2 = 9.9 \times 10^{-4} \ll 1$, the Eq.(17) for small beam size limit gives a good estimation near the detector for $P_{3bo} = P_{2b}(s_2 \rightarrow s_3, \sigma_2 \rightarrow \sigma_3, z_2 \rightarrow z_3)$. Compared with Eq.(15), we have P_{3bo} as indicated in Fig.5(b),

$$P_{3bo} = P_{2b}(s_2 \rightarrow s_3 = 3mm, \sigma_2 \rightarrow \sigma_3 = 4\mu m, z_2 \rightarrow z_3 = 2m) = 0.00042584 \quad (18)$$

$$P_{3bo} \approx \frac{\sigma_1\sigma_3}{d_L} \exp\left(-\frac{\sigma_1^2}{2d_1^2} (s_3 - s_1)^2\right) = 0.00251 \times 0.16922 = 0.0004253$$

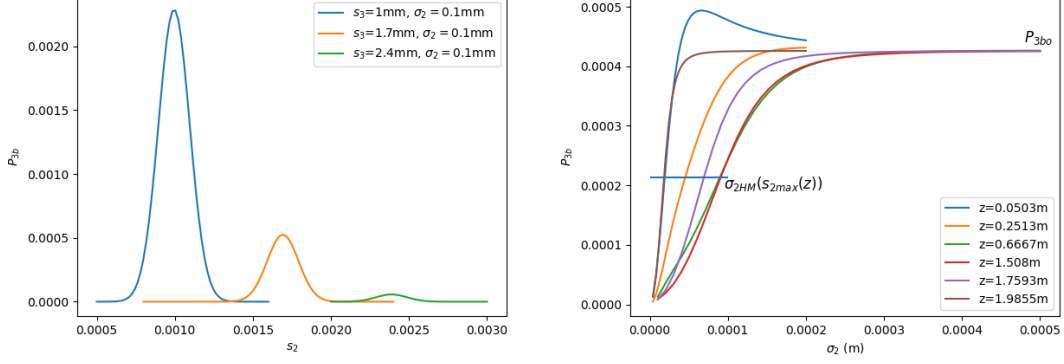


FIG. 5. (a) Plot P_{3b} vs. s_2 for various s_3 to find where P_{3b} reaches maximum for a fixed $\sigma_1 = 0.1\text{mm}$, $\sigma_2 = 0.1\text{mm}$, $\sigma_3 = 4\mu\text{m}$, $z = 0.666\text{m}$, $z_3 = 2\text{m}$, $s_1 = 0$ (b) Plot P_{3b} vs. σ_2 for various z with $s_2 = s_{2max}(z)$ set at where P_{3b} is maximized for any given σ_2 , $\sigma_1 = 50\mu\text{m}$, $s_1 = 0$, $s_3 = 3\text{mm}$, $\sigma_3 = 4\mu\text{m}$, $z_3 = 2\text{m}$

In Fig. 5(b) a horizontal line at $P_{3b}(\sigma_2, z) = \frac{1}{2}P_{3bo}$ shows where the curves for various slit 2 positions z cross the line, i.e., the corresponding $\sigma_{2HM}(s_{2max}(z))$. We observe that the half-maximum width $\sigma_{2HM}(s_{2max}(z))$ at crossing point $z = 0.05\text{m}$ is small; it increases to maximum as z increases from 0.25m to 1.5m , then decreases to about the same size as 0.05m at $z = 1.96\text{m}$. So we expect it will form a spindle shape when we plot $\sigma_{2HM}(s_{2max}(z))$ vs. z in Fig.2.

We numerically solved the equation $P_{3b}(\sigma_2, z) = \frac{1}{2}P_{3bo}$ for $\sigma_{2HM}(s_{2max}(z))$, and plot $s_{2max}(z)$ and $s_{2max}(z) \pm \sigma_{2HM}(s_{2max}(z))$ vs. z for $s_3 = 0, 1\text{mm}, 3\text{mm}$ in Figure 2 in the Introduction. There are single-particle wave packets emitted from the origin that propagate towards different directions; each of them forms a spindle-shaped region and finally converges into different detectors located at $s_3 = 0, 1\text{mm}, 3\text{mm}$ respectively. They do not create a cylindrical wave originating from the initial point at $z = 0$ as expected from the wave function $\psi_{2a}(x, z)$ given in Eq.(13) for the 2D case. This is just as in the 3D case, where we would expect a spherical wave to originate from a point for a single particle.

From the experimental setup in Fig. 1, we see that $\psi_{2a}(x, z)$ represents free space wave function propagation emitted from slit 1. From the probability amplitude $\psi_{2a}(x, z)$ in Eq.(13), we find

$$|\psi_{2a}(x_2, z)|^2 = \frac{\sqrt{2}e^{-\frac{\sigma_1^2(x_2-s_1)^2}{2(d_1^2+\sigma_1^4)}} \left| \frac{\sigma_1^2}{\Delta_1} \right|}{2\sqrt{\pi}\sqrt{|\sigma_1^2|}} \quad (19)$$

Hence the RMS width of $|\psi_{2a}(x_2, z)|^2$ is $\sigma_{2a} = \sqrt{\frac{d_1^2 + \sigma_1^4}{\sigma_1^2}}$ where $d_1 = \frac{\lambda z}{4\pi}$, it is plotted in Fig. 2 as a comparison with $\sigma_{2HM}(s_{2max}(z))$ showing it is entirely different. The width σ_{2a} is narrow at the origin $z = 0$, it monotonically increases as z increases, and at slit 3, it is widespread. The probability amplitude $\psi_{2a}(x_2, z)$ represents an ensemble, a distribution of individual events of single particle emissions represented by $s_{2max}(z) \pm \sigma_{2HM}(s_{2max}(z))$. As a comparison, $s_{2max}(z)$ and $s_{2max}(z) \pm \sigma_{2HM}(s_{2max}(z))$ vs. z represent a specific individual event for any given s_3 .

$\sigma_{2HM}(s_{2max}(z))$ provides an entirely different description of the single particle propagation between two points from that given by σ_{2a} derived from $\psi_{2a}(x_2, z)$. However, because the aperture slit 2 disturbs the single particle wave function, this description is approximate, and details such as the phase information of the wave function evolution between the slits are lost. Hence we need to reduce the effect of the slit 2 by replacing it with a perturbation, e.g., by a pin parallel to the y -axis to block the wave function from passing through it, as we outlined in the introduction. In the following section, we first calculate the perturbative effect of the pin.

4. PERTURBATIVE FUNCTION $\frac{\delta}{\delta f_2(x_2)}P_{3b}$, ITS INTEGRAL $\frac{1}{2} \int_{-\infty}^{\infty} dx_2 \frac{\delta}{\delta f_2(x_2, z_2)}P_{3b}$ AND ITS PHYSICAL MEANING

4.1 Calculate the contribution to final detection at a point between source and detection points

We calculate the contribution to P_{3b} of point 2 between source point 1 and detection point 3 according to the setup in Fig. 1. We apply the formulas in Section 2, we have

$$P_{3b} = \int_{-\infty}^{\infty} dx_3 |\psi_{3b}(x_3)|^2 \quad (20)$$

$$\psi_{3b}(x_3) = f_3(x_3) \int_{-\infty}^{\infty} dx_2 G(x_3, x_2; t_3 - t_2) f_2(x_2) \int_{-\infty}^{\infty} dx_1 G(x_2, x_1; t_2 - t_1) f_1(x_1)$$

Thus, we consider P_{3b} a functional of the function $f_2(x_2)$ when we use a pin with width δx_2 to block the wave function at position (x_2, z_2) . Let $f_2(x_2) = 1$ everywhere. The contribution of the section δx_2 to P_{3b} is given by the functional derivative of P_{3b} as $\frac{\delta}{\delta f_2(x_2)}P_{3b}\delta x_2$, hence the effect of the pin is $\delta P_{3b} = -\frac{\delta}{\delta f_2(x_2)}P_{3b}\delta x_2$. Hence, we can measure $\frac{\delta}{\delta f_2(x_2)}P_{3b}$ using the pin blocking. We have

$$\begin{aligned} \frac{\delta}{\delta f_2(x_2)}P_{3b} &= \frac{\delta}{\delta f_2(x_2)} \int dx_3 |\psi_{3b}(x_3)|^2 = \int dx_3 \frac{\delta}{\delta f_2(x_2)} \psi_{3b}(x_3) \psi_{3b}^*(x_3) \\ &= \int dx_3 \left(f_3(x_3) G(x_3, x_2; t_3 - t_2) \int_{-\infty}^{\infty} dx_1 G(x_2, x_1; t_2 - t_1) \psi_1(x_1) \right) \psi_{3b}^*(x_3, z_3) + c.c. \\ &= \left(\int dx_3 \psi_{3b}^*(x_3, z_3) f_3(x_3) G(x_3, x_2; t_3 - t_2) \right) \int_{-\infty}^{\infty} dx_1 G(x_2, x_1; t_2 - t_1) \psi_1(x_1) + c.c. \end{aligned}$$

Since $f_2(x_2) = 1$, we recognize that without slit 2, $\psi_{3b}(x_3, z_3)$ here can be written as $\psi_{2b}(s_2 \rightarrow s_3, \sigma_2 \rightarrow \sigma_3, z_2 \rightarrow z_3)$, similar to P_{3bo} we discussed in Section 3.2. Because in this expression $\frac{\delta P_{3b}}{\delta f_2(x)}$, the slit 2 has been replaced by a point x_2 , and $f_2(x_2)$ is already removed by the differentiation, the experiment is equivalent to an experiment where the slit 2 is moved to replace slit 3. To be able to apply the formula for $\psi_{2a}(x)$ and $\psi_{2b}(x)$ in Eq.(13) to simplify the derivation, we replace all the subscripts 3 by 2 in the expression above and replace x_2, z_2 , by x, z , and denote the pin function as $\chi(x)$, while using $f_2(x_2)$ to replace $f_3(x_3)$ as follows

$$\begin{aligned} \frac{\delta P_{3bo}}{\delta \chi(x)} &= \phi_b(x) \psi_{2a}(x) + c.c. \quad (21) \\ \psi_{2a}(x) &\equiv \int dx_1 G(x, x_1; t) \psi_1(x_1) \\ \phi_b(x) &\equiv \int dx_2 \psi_{2b}^*(x_2, z_2) f_2(x_2) G(x_2, x; t_L - t) \end{aligned}$$

Here we define another function $\phi_b(x_2)$, it represents the propagation from point x to x_2 , with the slit 2 function $f_2(x_2)$ replaced by $\psi_{2b}^*(x_2, z_2) f_2(x_2)$. We let $x_2 = x_3, s_2 = s_3, \sigma_2 = \sigma_3, z_2 = z_3 = L$, and we have taken $t_2 - t_1 \equiv t = z/v$ and $t_3 - t_2 = t_L - t = (L - z)/v$, and the pin position is (x, z) . Because now the function $f_2(x_2)$ is used to represent and replace the original $f_3(x_3)$, we need to replace the original $f_2(x_2)$ by $\chi(x) = 1$.

With this understanding, $\frac{\delta P_{3bo}}{\delta \chi(x)}$ **and** $\frac{\delta P_{3b}}{\delta f_2(x_2)}$ **represent the same function with different notation.** Notice that during the derivation of $\frac{\delta P_{3bo}}{\delta \chi(x)}$, x, z are different from $x_2, z_2 = x_3, z_3$. x, z are the positions of the blocking pin,

while $x_2, z_2 = x_3, z_3$ are the positions of the exit slit position. The notation $\frac{\delta P_{3bo}}{\delta \chi(x)}$ is convenient for derivation, while the notation $\frac{\delta P_{3b}}{\delta f_2(x_2)}$ is convenient for discussion when compared with the experiment setup in Fig. 1.

From this expression, we see that $\frac{\delta}{\delta f_2(x_2)} P_{3b}$ is closely related to Green's function $G(x_3, x_2; t_3 - t_2)G(x_2, x_1; t_2 - t_1)$; it is the product of the two Feynman propagators and represents the path integral from x_1 to x_3 passing through point x_2 , or in other words, the corresponding probability amplitude.

$$4.2 \text{ The relation between } \frac{\delta P_{3bo}}{\delta \chi(x)} \text{ and } P_{3bo}, P_{3bo} = \frac{1}{2} \int_{-\infty}^{\infty} dx \frac{\delta P_{3bo}}{\delta \chi(x)},$$

From Eq.(21) we have

$$\begin{aligned} \int_{-\infty}^{\infty} dx \frac{\delta P_{3bo}}{\delta \chi(x)} &= \int_{-\infty}^{\infty} dx \int_{-\infty}^{\infty} dx_2 \psi_{2b}^*(x_2, z_2) f_2(x_2) G(x_2, x; t_L - t) \int_{-\infty}^{\infty} dx_1 G(x, x_1; t) \psi_1(x_1) + c.c. \\ &= \int_{-\infty}^{\infty} dx_2 \psi_{2b}^*(x_2, z_2) f_2(x_2) \int_{-\infty}^{\infty} dx_1 \int_{-\infty}^{\infty} dx G(x_2, x; t_L - t) G(x, x_1; t) \psi_1(x_1) + c.c. \\ &= \int_{-\infty}^{\infty} dx_2 \psi_{2b}^*(x_2, z_2) f_2(x_2) \int_{-\infty}^{\infty} dx_1 G(x_2, x_1; t_L) \psi_1(x_1) + c.c. \\ &= \int_{-\infty}^{\infty} dx_2 \psi_{2b}^*(x_2, z_2) \psi_{2b}(x_2, z_2) + c.c. = \int_{-\infty}^{\infty} dx_2 |\psi_{2b}(x_2)|^2 + c.c. = P_2 + c.c. = 2P_{2b} = 2P_{3bo} \end{aligned} \quad (22)$$

Thus we have a simple relation between $\frac{\delta}{\delta \chi(x)} P_{3bo}$ and P_{3bo} ,

$$P_{3bo} = \frac{1}{2} \int_{-\infty}^{\infty} dx \frac{\delta P_{3bo}}{\delta \chi(x)} \quad (23)$$

Thus, $\int_{-\infty}^{\infty} dx \frac{\delta P_{3bo}}{\delta \chi(x)}$ is independent of $z = vt$, it is a constant, i.e., twice the probability of a particle passing through the exit slit 3. Notice that we denote the pin position as (x, z) . $P_{3bo} = \frac{1}{2} \int_{-\infty}^{\infty} dx \frac{\delta P_{3bo}}{\delta \chi(x)}$ is independent from z , meaning immediately after passing through the entrance slit, the integral of $\frac{1}{2} \int_{-\infty}^{\infty} dx \frac{\delta P_{3bo}}{\delta \chi(x)}$ has already been determined as P_{3bo} at the exit. This result confirms the discussion in the Introduction about the process of wave function collapse.

We consider the slit function as Gaussian because the derivation of the analytical expression is simple for a single slit. For multiple detectors on the exit screen, the function for different slits will have an overlap that is not negligible unless their separation is much larger than σ_3 . We can replace the Gaussian slit function $f_3(x_3) = \exp(-\frac{1}{2\sigma_3^2}(x_3 - s_3)^2)$ with a hard-edged slit when the slit width is small:

$$P_{3bo}(s_3) = \int dx_3 \exp(-\frac{1}{2\sigma_3^2}(x_3 - s_3)^2) |\psi_{2a}(x_3)|^2 \approx |\psi_{2a}(s_3)|^2 \sqrt{2\pi}\sigma_3, \quad (24)$$

i.e., we can replace $f_3(x_3)$ by a hard edge slit of width $\Delta x_3 = \sqrt{2\pi}\sigma_3$. The condition of this approximation is $\sqrt{2\pi}\sigma_3 \ll \sigma_{2a}$, where $\sigma_{2a} = \sqrt{\frac{d_1^2 + \sigma_1^4}{\sigma_1^2}}$ is in Eq.(19). Notice that P_{3bo} here is P_{3b} with slit 2 wide open, equivalent to P_{2b} with $s_2 = s_3, \sigma_2 = \sigma_3, z_2 = z_3$, as we discussed in Sections 3 and 4.1. So a Gaussian function slit of width σ_3 is equivalent to a hard edge slit of width $\sqrt{2\pi}\sigma_3$. If σ_3 is sufficiently small, the detection probability per unit length of s_3 is $\frac{P_{3bo}(s_3)}{\sqrt{2\pi}\sigma_3}$.

For a hypothetical experiment, we may consider an infinite set of slits $\{s_{3n}\}$, each with width Δs_{3n} extending over the exit screen. In the limit $\sigma_3 \rightarrow 0, \Delta s_{3n} \rightarrow 0$, the total probability over the sum of all these slits is

$$\lim_{\sigma_3 \rightarrow 0} \lim_{\Delta s_{3n} \rightarrow 0} \sum_n \frac{\Delta s_{3n}}{\sqrt{2\pi\sigma_3}} P_{3bo}(s_{3n}) = \int dx_3 |\psi_{2a}(x_3)|^2 \int \frac{ds_{3n}}{\sqrt{2\pi\sigma_3}} \exp\left(-\frac{1}{2\sigma_3^2}(x_3 - s_{3n})^2\right) = \int dx_3 |\psi_{2a}(x_3)|^2 = 1 \quad (25)$$

For each $s_{3n}, P_{3bo}(s_{3n}) = \frac{1}{2} \int_{-\infty}^{\infty} dx \frac{\delta P_{3bo}(s_{3n})}{\delta \chi(x)}$ gives the probability of the particle passing through the slit s_{3n} . Thus, $\psi_{2a}(x_3)$ represents the probability amplitude of the particle distribution. As a comparison, $\frac{\delta P_{3bo}(s_{3n})}{\delta \chi(x)}$ represents an individual single particle that eventually passes through the slit at s_{3n} . The fact that $P_{3bo}(s_{3n}) = \frac{1}{2} \int_{-\infty}^{\infty} dx \frac{\delta P_{3bo}(s_{3n})}{\delta \chi(x)}$ is independent of z even though $\frac{\delta P_{3bo}(s_{3n})}{\delta \chi(x)}$ does depend on z , means that even at the beginning at $z = 0_+$, the specific sampling from the distribution represented by $\psi_{2a}(x_3)$ has already realized.

We shall use this independence from z to simplify the derivation of $\frac{\delta}{\delta \chi(x)} P_{3bo} = \frac{\delta P_{3bo}}{\delta \chi(x)} = \phi_b(x) \psi_{2a}(x) + c.c.$ in the next section 4.3.

4.3 The perturbative function $\frac{\delta}{\delta \chi(x)} P_{3bo}$

We emphasize that even though we used the notation of $\frac{\delta}{\delta f_2(x_2)} P_{3b}$ in the introduction as a function of x_2 , it is the same function $\frac{\delta P_{3bo}}{\delta \chi(x)}$ as a function of x used here to simplify derivation because P_{3bo} has the same expression as P_{2b} which is much simpler than P_{3b} .

We first need to express $\psi_{2b}(x)$ and $\psi_{2a}(x)$ in terms of the parameters of the experimental setup more directly. We have $\ln \psi_{2b}(x_2, z_2)$ in Eq.(13),

$$\ln \psi_{2b}(x_2, z_2 = L) = \alpha_{2b}(x_2 - s_{2b})^2 + c_{2b} = -\frac{1}{4\Delta_1} \frac{\Delta_1 + \sigma_2^2}{\sigma_2^2} (x_2 - s_{2b})^2 - \frac{(s_1 - s_2)^2}{4(\Delta_1 + \sigma_2^2)} + \frac{1}{2} \ln \left(\frac{\sigma_1^2}{\Delta_1} \right) + \frac{1}{4} \ln \left(\frac{1}{2\pi\sigma_1^2} \right) \quad (26)$$

$$\Delta_1 = \sigma_1^2 + id_1, d_1 = \frac{\lambda(z_2 - z_1)}{4\pi} = \frac{\lambda L}{4\pi}$$

Because $f_2(x_2), \alpha_{f_2}, \beta_2, d_2$ are the same as given in section 2.2, i.e., $f_2(x_2) = \exp(\alpha_{f_2}(q_2 - s_2)^2), \alpha_{f_2} \equiv -\frac{1}{4\sigma_2^2}, \beta_2 = \frac{1}{4d_2}, d_2 = \frac{\lambda(L-z)}{4\pi}$, we have

$$\begin{aligned} \ln f_2(x_2) G(x_2, x; t_2 - t) &= \alpha_{f_2}(x_2 - s_2)^2 + i\beta_2(x_2 - x)^2 + \frac{1}{2} \ln \frac{\beta_2}{i\pi} \\ \ln \psi_{2b}^*(x_2, z_2) f_2(x_2) G(x_2, x; t_L - t) &= \alpha_{f_2}(x_2 - s_2)^2 + i\beta_2(x_2 - x)^2 + \overline{\alpha_{2b}}(x_2 - \overline{s_{2b}})^2 + \frac{1}{2} \ln \frac{\beta_2}{i\pi} + \overline{c_{2b}} \\ &= (\alpha_{f_2} + i\beta_2 + \overline{\alpha_{2b}}) x_2^2 - 2(\alpha_{f_2} s_2 + i\beta_2 x + \overline{\alpha_{2b}} \overline{s_{2b}}) x_2 + \alpha_{f_2} s_2^2 + i\beta_2 x^2 + \overline{\alpha_{2b}} \overline{s_{2b}}^2 + \frac{1}{2} \ln \frac{\beta_2}{i\pi} + \overline{c_{2b}} \end{aligned} \quad (27)$$

Apply the Gaussian integral $\int dx \exp(ax^2 + bx + c) = \exp\left(-\frac{b^2}{4a} + c + \ln\left(\frac{\pi}{-a}\right)^{\frac{1}{2}}\right)$,

$$\ln \phi_b(x) = \ln \int dx_2 \psi_{2b}^*(x_2, z_2) f_2(x_2) G(x_2, x; t_2 - t)$$

$$\ln \phi_b(x) = \alpha_{f_2} s_2^2 + i\beta_2 x^2 + \frac{1}{2} \ln \frac{\beta_2}{i\pi} + \ln \left(\frac{\pi}{-(\alpha_{f_2} + i\beta_2 + \overline{\alpha_{2b}})} \right)^{\frac{1}{2}} + \overline{\alpha_{2b}} s_{2b}^2 + \overline{c_{2b}} - \frac{4(\alpha_{f_2} s_2 + i\beta_2 x + \overline{\alpha_{2b}} s_{2b})^2}{4(\alpha_{f_2} + i\beta_2 + \overline{\alpha_{2b}})} \quad (28)$$

and because in $\psi_{2a}(x) \equiv \int dx_1 G(x, x_1; t) \psi_1(x_1)$, the propagation distance from the entrance slit to the pin is z , not z_2 , we need to replace $\Delta_1 = \sigma_1^2 + id_1$ by $\Delta = \sigma_1^2 + id$ as defined in the following, and we have

$$\ln \psi_{2a}(x) = \frac{\ln \left(\frac{1}{2\pi\sigma_1^2} \right)}{4} + \frac{\ln \left(\frac{\sigma_1^2}{\Delta} \right)}{2} - \frac{(x - s_1)^2}{4\Delta} \quad (29)$$

$$\Delta = \sigma_1^2 + id, d = \frac{\lambda z}{4\pi},$$

Since $\ln \phi_b(x)$ and $\ln \psi_{2a}(x)$ are both quadratic forms of x , $\phi_b(x)\psi_{2a}(x)$ is Gaussian. we can write $\ln \phi_b(x)\psi_{2a}(x)$ in the quadratic form as

$$\ln \phi_b(x)\psi_{2a}(x) = \alpha_\chi (x - x_c)^2 + C$$

$$\alpha_\chi = i\beta_2 - A(i\beta_2)^2 - \frac{1}{4\Delta}$$

$$x_c = \frac{(A_2 i\beta_2 (\alpha_{f_2} s_2 + \overline{\alpha_{2b}} s_{2b}) - s_1 \frac{1}{4\Delta})}{\alpha_\chi} \quad (30)$$

$$C = -\frac{(A_2 i\beta_2 (\alpha_{f_2} s_2 + \overline{\alpha_{2b}} s_{2b}) - s_1 \frac{1}{4\Delta})^2}{\alpha_\chi} - A_2 (\alpha_{f_2} s_2 + \overline{\alpha_{2b}} s_{2b})^2 - \frac{(s_1)^2}{4\Delta} + \alpha_{f_2} s_2^2$$

$$+ \frac{1}{2} \ln \frac{\beta_2}{i\pi} + \ln \left((-\pi A_2)^{\frac{1}{2}} \right) + \overline{\alpha_{2b}} s_{2b}^2 + \overline{c_{2b}} + \frac{\ln \left(\frac{1}{2\pi\sigma_1^2} \right)}{4} + \frac{\ln \left(\frac{\sigma_1^2}{\Delta} \right)}{2}$$

$$A \equiv \frac{1}{\alpha_{f_2} + i\beta_2 + \overline{\alpha_{2b}}}$$

where we introduce A to simplify the writing. Thus we have

$$\frac{\delta P_{3bo}}{\delta \chi(x)} = \phi_b(x)\psi_{2a}(x) + c.c. \quad (31)$$

$$= \exp(\alpha_\chi (x - x_c)^2 + C) + c.c.$$

Where α_χ and x_c are identified by completing the quadratic form and simplified in Appendix IV. To make writing simpler, we define the dimensionless parameter of distance ratio ξ as follows: we find

$$\alpha_\chi = -\frac{1}{2\sigma_1^2} \frac{i\mu(\mu^2 + \rho\mu^2 + 1)}{(-i\mu + \xi)(\mu(i\xi - \mu)\rho + 2(\xi - 1)(i\mu + 1))} \quad (32)$$

$$\xi \equiv \frac{d}{d_1} = \frac{z}{L}$$

where μ, ρ are defined in Eq.(16). And

$$\begin{aligned} x_c &= \frac{c_{S1}s_1 + c_{S2}s_2}{\mu^2 + \rho\mu^2 + 1} \\ c_{S1} &\equiv \rho\mu^2 - (i\mu + 1)(\xi - 1) \\ c_{S2} &\equiv (\mu - i)(\mu + i\xi) \end{aligned} \quad (33)$$

To simplify C in Eq.(30), we apply the Gaussian integral Eq.(9), the formula of P_{2b} Eq.(16), and $P_{3bo} = \frac{1}{2} \int_{-\infty}^{\infty} dx \frac{\delta P_{3bo}}{\delta \chi(x)}$, and we have

$$\begin{aligned} \frac{1}{2} \int_{-\infty}^{\infty} dx \frac{\delta P_{3bo}}{\delta \chi(x)} &= \frac{1}{2} \int_{-\infty}^{\infty} dx \exp(\alpha_\chi (x - x_c)^2 + C) + c.c. \\ &= \exp(C) \sqrt{\frac{\pi}{-\alpha_\chi}} = P_{2b} = \sqrt{\frac{\rho\mu^2}{\mu^2 + \rho\mu^2 + 1}} \exp\left(-\frac{1}{2\sigma_1^2} \frac{\mu^2}{\mu^2 + \rho\mu^2 + 1} (s_1 - s_2)^2\right) \\ C &= -\frac{1}{2\sigma_1^2} \frac{\mu^2}{\mu^2 + \rho\mu^2 + 1} (s_1 - s_2)^2 + \ln \sqrt{\frac{\rho\mu^2}{\mu^2 + \rho\mu^2 + 1}} + \ln \frac{\sqrt{-\alpha_\chi}}{\sqrt{\pi}} \end{aligned} \quad (34)$$

Compared with C given in Eq.(30), we can separate the terms quadratic in s_1, s_2 and the logarithmic terms in C in Eq.(30). This separation simplifies the calculation to confirm that the complicated expression C in Eq.(30) can be simplified significantly as the sum of the following 3 terms:

$$\ln \frac{\sqrt{-\alpha_\chi}}{\sqrt{\pi}} + \ln \sqrt{\frac{\rho\mu^2}{\mu^2 + \rho\mu^2 + 1}} = \frac{1}{2} \ln \frac{\beta_2}{i\pi} + \ln \left((-\pi A)^{\frac{1}{2}} \right) + \frac{\ln \left(\frac{\sigma_1^2}{\Delta} \frac{\sigma_1^2}{\Delta_1} \frac{1}{2\pi\sigma_1^2} \right)}{2} \quad (35)$$

$$\begin{aligned} -\frac{1}{2\sigma_1^2} \frac{\mu^2}{\mu^2 + \rho\mu^2 + 1} (s_1 - s_2)^2 &= -\frac{(Ai\beta_2(\alpha_{f2}s_2 + \overline{\alpha_{2b}s_{2b}}) - s_1 \frac{1}{4\Delta})^2}{\alpha_\chi} \\ -A(\alpha_{f2}s_2 + \overline{\alpha_{2b}s_{2b}})^2 - \frac{(s_1)^2}{4\Delta} + \alpha_{f2}s_2^2 + \overline{\alpha_{2b}s_{2b}}^2 - \frac{(s_1 - s_2)^2}{4(\overline{\Delta_1} + \sigma_2^2)} \end{aligned} \quad (36)$$

Substituting C in Eq.(31) by the expression of C in Eq.(34), and using the expression of P_{2b} in Eq.(34), then replacing P_{2b} by P_{3bo} , the result is the analytical expression for $\frac{\delta P_{3bo}}{\delta \chi(x)}$,

$$\frac{\delta P_{3bo}}{\delta \chi(x)} = P_{3bo} \frac{\sqrt{-\alpha_\chi}}{\sqrt{\pi}} \exp(\alpha_\chi (x - x_c)^2) + c.c. \quad (37)$$

4.4 Compare the plot of $\frac{\delta}{\delta f_2(x_2)} P_{3b}$ with $Re(\psi_{2a}(x, z))$, $|\psi_{2a}(x, z)|^2$, centroid x_{c0} and fringe spacing x_π , peak x_{max} and width σ_w of the envelope of $\frac{\delta}{\delta f_2(x_2)} P_{3b}$

For the example of setup with $s_1 = 0.0$, $\sigma_1 = 50\mu m$, $\sigma_3 = 4\mu m$, $z_3 = 2m$, we plot $\frac{\delta P_{3b}}{\delta f_2(x)}$ for several pin positions z compared with $Re(\psi_{2a}(x, z))$, $|\psi_{2a}(x, z)|^2$ in Fig.6. Fig.6(a,b,c) is for $s_3 = 3mm$, $z = 0.7m, 1.7m, 1.98m$. The example

of $z = 1.95m$, $s_3 = 3mm$ is given in Fig.3(a). $\frac{\delta P_{3b}}{\delta f_2(x)}$ vs. x, z in color scale for $s_3 = 3mm$ is given in Fig. 3(b) in the introduction.

The blue vertical line is the centroid of the wave packet. The plots show that when $s_3 = 3mm$, $\frac{\delta P_{3bo}}{\delta f_2(x)}$ is a wave packet with its centroid moving from $x = 0, z = 0$ to $x = 3mm, z = 2m$. The wave packet has both amplitude and phase information. The centroid is where the phase is stationary, i.e., it is where the phase $\text{Im}(\alpha_\chi (x - x_c)^2)$ as the function of x has its derivative $\frac{\partial}{\partial x} \text{Im}(\alpha_\chi (x - x_c)^2) = 0$. Solving this equation, we find the stationary point is

$$x_{c0} = \frac{\alpha_{\chi i} x_{cr} + \alpha_{\chi r} x_{ci}}{\alpha_{\chi i}} = x_{cr} + \frac{\alpha_{\chi r}}{\alpha_{\chi i}} x_{ci} \quad (38)$$

Where $\alpha_{\chi r}, \alpha_{\chi i}, x_{cr}, x_{ci}$ are the real part and imaginary part of α_χ, x_c such that $\alpha_\chi = \alpha_{\chi r} + i\alpha_{\chi i}, x_c = x_{cr} + ix_{ci}$ as calculated from Eq.(32,33).

The phase of $\frac{\delta P_{3bo}}{\delta \chi(x)}$ as a function of x is given by to $\theta = \text{Im}(\alpha_\chi (x - x_c)^2)$, θ changes quadratically when x is away from the centroid x_{c0} , the further away from the x_{c0} , the faster it varies. To calculate the fringe spacing, we assume the points are spaced with a phase difference $\Delta\theta = n\pi$ from the centroid x_{c0}

$$\Delta\theta = \text{Im}\left(\left(\alpha_\chi (x_{c0} + \Delta x - x_c)^2\right) - \left(\alpha_\chi (x_{c0} - x_c)^2\right)\right) = n\pi \quad (39)$$

From this equation, we find $\Delta x = \pm x_\pi \sqrt{n}$ $x_\pi = \sqrt{\frac{\pi}{\alpha_{\chi i}}}$. For the example in Fig. 6(d), $x_{c0} \approx 2.970mm$ $\alpha_\chi \approx (-0.03268 + 3.1729i) \times 10^8 m^{-2}$, $x_\pi \approx 99.5\mu m$. We use the thin red lines to indicate the fringe spacing; they are not at peaks of the fringes because the phase of x_{c0} is not zero.

Using the same method, we find the position of the peak of the envelope of $\frac{\delta P_{3b}}{\delta f_2(x)}$, i.e., $|P_{3bo} \sqrt{\frac{-\alpha_\chi}{\pi}} \exp(\alpha_\chi (x - x_c)^2)|$ as $x_{max} = \frac{\alpha_{\chi r} x_{cr} - \alpha_{\chi i} x_{ci}}{\alpha_{\chi r}} = 2.878mm$ and its width $\sigma_w^2 = -\frac{1}{2\alpha_{\chi r}}$ with $\sigma_w = 392\mu m$ indicated by the blue lines in Fig. 6(d). We see that x_{c0} is not at the peak of the envelope of the green curve of $\frac{\delta P_{3b}}{\delta f_2(x)}$, and it is further away from the peak of the wave function $\psi_{2a}(x, z)$.

Fig. 3(b) and Fig. 6 show that $\frac{\delta P_{3b}}{\delta f_2(x)}$ represents a wave packet moving towards the exit slit, and when close to the exit point, the width σ_w becomes very small, and the fringe spacing x_π rapidly becomes very narrow and hardly visible, and hence becomes more difficult to measure.

For a comparison, the plot of $\text{Re}(\psi_{2a}(x, z))$ and $|\psi_{2a}(x, z)|^2$ are entirely different; the width increases as z increases until at the exit slit, where it is widespread. $\text{Re}(\psi_{2a}(x, z))$ has fringes, but we can only measure $|\psi_{2a}(x, z)|^2$.

We consider the well-known wave function $\psi_{2a}(x, z)$ to represent a cylindrical wave starting from the entrance slit and continuously spreading out until it finally arrives at the screen of the exit slit. Notice that the plots of $\text{Re}(\psi_{2a}(x, z))$ and $|\psi_{2a}(x, z)|^2$ in Fig. 6 and Fig. 2 do not show the cylindrical waveform explicitly because the phase represented in Fig. 6 is only the phase of $\psi(x, z)$ in $\phi(x, z, t) = \exp(i(kx - \omega_k t)) \psi(x, z)$ as defined in Section 2.1; it does not include the longitudinal phase $(kx - \omega_k t)$. The cylindrical waveform is implicitly exhibited only when we examine the waveform of $\text{Re}(\psi_{2a}(x, z))$ and see it spreading out as z increases from $z = 0.7m$ to $1.7m$ and $1.98m$. It would not be so easy to show the cylindrical waveform because, in a (z, x) 2D plot, the phase $(kx - \omega_k t)$ variation will dominate over the phase variation of the slow-varying amplitude and phase function $\psi(x, z)$ for a case where the paraxial approximation is valid. The curvature of the cylindrical wavefront becomes visible only when x is the same order as z . But we only consider those regions where $|x| \ll z$ in the paraxial approximation.

We discuss this cylindrical waveform here mainly because we would like to compare it to $\frac{\delta P_{3b}}{\delta f_2(x)}$ shown in Fig. 2, Fig. 3(b), and Fig. 6, where it exhibits an entirely different picture of wave packets emitted from the entrance slit into various directions and striking on the exit screen at different points. The wave packet width is very narrow at the entrance slit, grows wider and reaches maximum width, then becomes narrower again until it converges into the exit slit, forming a spindle-shaped region.

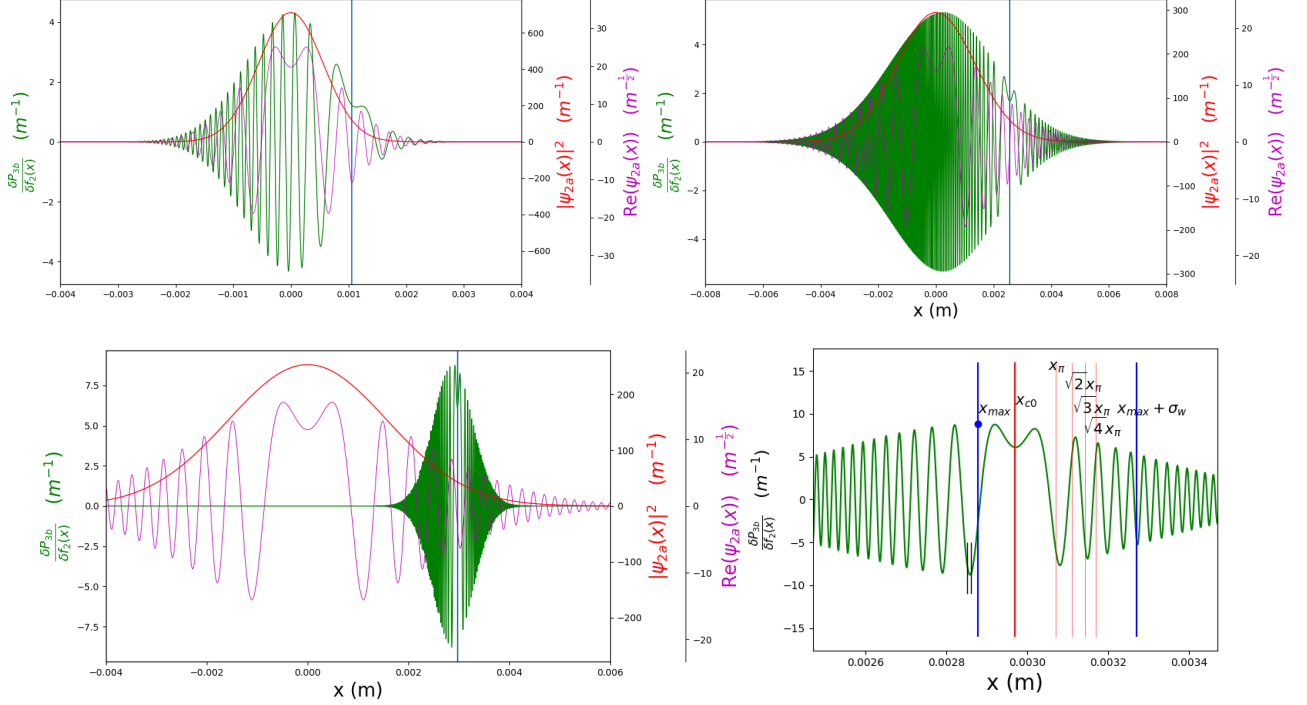


FIG. 6. Compare diffraction pattern $|\psi_{2a}(x_3, z_3)|^2$ perturbative function $\frac{\delta}{\delta f_2(x_2)} P_{3b}$ and $|\phi_b(x)\psi_{2a}(x)|$ of Eq.(31) (a) $s_3=3mm$, $z = 0.7m$, (b) $s_3=3mm$, $z = 1.7m$ (c) $s_3=3mm$, $z = 1.98m$. $s_1 = 0.0$, $\sigma_1 = 50\mu m$, $\sigma_3 = 4\mu m$, $z_3 = 2m$. The blue vertical line is the centroid x_{c0} of the wave packet. (d) same as (c) for region near $x_{c0} = 2.97mm$, indicates location of x_{max} , $x_{max} + \sigma_w$, and $x_{c0}, x_{c0} \pm x_\pi, x_{c0} \pm \sqrt{2}x_\pi, x_{c0} \pm \sqrt{3}x_\pi, x_{c0} \pm \sqrt{4}x_\pi$, with $x_\pi \approx 99.5\mu m$. $\sqrt{4}x_\pi - \sqrt{3}x_\pi = 26.7\mu m$

4.5 The small slit size limit

It would be interesting to study the small slit size limit because in this limit whether the profile of the entrance slit and exit slit are Gaussian or hard edge is no longer important. But when we try to work out the calculation replacing the Gaussian functions f_1, f_3 by δ -functions, we have some difficulties because P_{3b} and $\frac{\delta}{\delta f_2(x_2)} P_{3b}$ become zero. Then, we first work out the expression for $\frac{\delta}{\delta f_2(x_2)} P_{3b}$, and now we take this limit. We will show in the following that the ratio $\rho = \frac{\sigma_2^2}{\sigma_1^2}$ is relevant.

The example we have for Fig.2-4 all have small σ_1 and σ_2 , where $\mu = \frac{\sigma_1^2}{d_1} = \frac{4\pi\sigma_1^2}{\lambda L} \ll 1$, If z is not very close to 0 or L so $\xi = \frac{z}{L}$ and $1 - \xi = \frac{L-z}{L}$ is too far from order of magnitude 1, we can take the approximation in Eq.(32)

$$\alpha_\chi = \alpha_{\chi r} + i\alpha_{\chi i} \approx -\frac{\mu^2}{2\sigma_1^2} \frac{(\rho\xi^2 + 2(\xi - 1)^2)}{4\xi^2(\xi - 1)^2} - i\frac{\mu}{4\sigma_1^2} \frac{1}{\xi(\xi - 1)} \quad (40)$$

We find the phase shift π width $x_\pi = \sqrt{\frac{\pi}{\alpha_{\chi i}}} \approx \sqrt{\lambda L \xi(1 - \xi)}$. This width is shown in Fig. 7 as the spindle-shaped region of $\frac{\delta P_{3bo}}{\delta \chi(x)}$ reaches maximum at $z = L/2$ in the middle of slits 1 and 2. The wave packet envelope

width is also given in Fig. 7 as $\sigma_w \approx \frac{\lambda L}{2\sqrt{2\pi}\sigma_1} \sqrt{\frac{\xi^2(\xi - 1)^2}{\frac{\rho}{2}\xi^2 + (\xi - 1)^2}}$. The maximum of σ_w is the root of a cubic equation

$\rho\xi^3 + 2\xi^3 - 6\xi^2 + 6\xi - 2 = 0$, indicated by a vertical blue line. Fig. 7 shows the width x_π and σ_w of the wave packet $\frac{\delta}{\delta f_2(x_2)} P_{3b}$ in the small slit size limit agrees with the formula in Eq.(32) well.

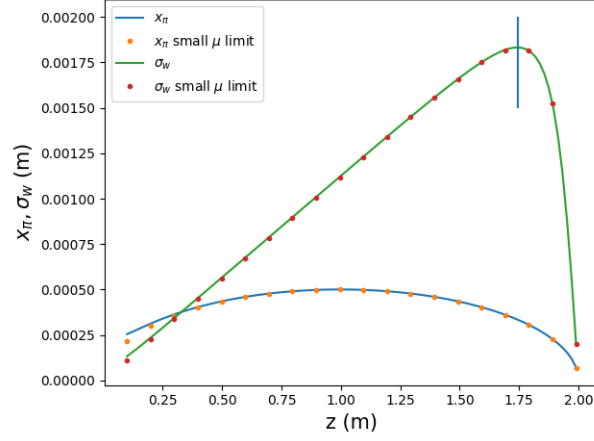


FIG. 7. width x_π, σ_w calculated from Eq.(32) compared with the limit $\sigma_1, \sigma_2 \rightarrow 0$. The maximum width x_π of phase shift π is in the middle point $z = 1m$, and the maximum of the wave packet envelope is at $z = 1.743m$ indicated by the blue vertical line corresponding to the solution of the cubic equation $\xi = z/L = 0.872$.

The result shows the relative position $\xi = z/L$ of maximum width σ_w depends on $\rho = \frac{\sigma_2^2}{\sigma_1^2}$, so it is not in the middle like the position of maximum x_π always in the middle.

However, since $P_{3bo} = \frac{1}{2} \int_{-\infty}^{\infty} dx \frac{\delta P_{3bo}}{\delta \chi(x)}$, contribution to P_{3bo} mainly comes from near x_{c0} . Far from x_{c0} , $\frac{\delta P_{3bo}}{\delta \chi(x)}$ oscillates fast, and the positive and negative peaks cancel each other. Hence, the width x_π is more relevant to the total probability P_{3bo} than the envelope width σ_w . Thus, the spindle-shaped region visible in Fig. 2 and Fig. 3(b) is mainly determined by the spindle-shaped curve of x_π in Fig.7. When one examines Fig. 3(b) in detail, it is also possible to observe the shape of the curve σ_w in Fig. 3(b).

4.6 Counting number and relation to measurement error bar

Take a point in Fig. 6(d), at $x = 2.859mm$, and take a width $\Delta x = 10\mu$ to represent the blocking pin indicated by the two vertical lines in the figure. $\frac{\delta P_{3b}}{\delta f_2(x)} \approx -8.58m^{-1} \pm 0.18$ within this $10\mu m$. $P_{3b} = 0.0004258$ is already calculated in Section 3.2 for the same set of parameters as Fig. 9(d). The contribution of Δx to the final probability is $\frac{1}{P_{3b}} \frac{\delta P_{3b}}{\delta f_2(x)} \Delta x \approx \frac{-8.58/m}{0.0004258} \times 10\mu m = -0.20$. If we block a line of width Δx that passes through x (this line is in parallel in the y -direction) such that immediately behind this line $\psi(x) = 0$, then the probability of passing through the end slit 3 will decrease by a factor of -0.20 , i.e., the probability will increase by a factor of 1.20.

To get sufficient accuracy, we use the Poisson distribution formula $P(k) = \frac{n^k e^{-n}}{k!}$, its RMS is \sqrt{n} where n is the mean rate of events during a fixed interval.

If we take the recorded detection count $n = 4 \times 10^4$, then the RMS fluctuation is $\Delta n = \sqrt{n} = 200$, $\frac{\Delta n}{n} = 0.005$, and the probability of detection when normalized as 1 without blocking is increased from 1 to 1.20 ± 0.005 . Thus the error of the measurement $\frac{\delta P_{3b}}{\delta f_2(x)}$ is $0.005/0.2 = 0.025$. The error due to the variation of $\frac{\delta P_{3b}}{\delta f_2(x)}$ within the pin width is $0.18/8.58 = 0.02$. There is a trade-off between these two different error types when choosing the pin width.

We restrict our discussion to the fundamental principles of the experiment, where we have assumed a detection quantum efficiency of 100%, omitting further details. In reality, the lower detector quantum efficiency may correspond to taking a smaller σ_3 , while the stability of the system and the background noise may be more important for the precision of the measurement.

5. WAVE PACKET PROPAGATION IN AN INTERFERENCE EXPERIMENT

To demonstrate the phase information inherent in $\frac{\delta}{\delta\chi(x)}P_{3bo}$, we study an interference experiment as shown in Fig. 4. We replace the single entrance slit 1 in Fig. 1 with two slits. To keep coherence between the two slits, the wavefront is assumed to arrive at the two slits in phase. The initial wave function at the two slits is set the same except with a transverse displacement of $2s_1$,

$$\begin{aligned}\psi_1(x_1) &= \frac{(\psi_{1+}(x_1) + \psi_{1-}(x_1))}{\sqrt{2}} \\ \psi_{1\pm}(x_1) &= f_1(x_1 \mp s_1) = \left(\frac{1}{2\pi\sigma_1^2}\right)^{\frac{1}{4}} \exp\left(-\frac{1}{4\sigma_1^2}(x_1 \mp s_1)^2\right)\end{aligned}\quad (41)$$

They centered at $s_1 = 1mm$ and $s_1 = -1mm$ respectively, and are in phase. Their separation $2s_1 \gg \sigma_1$, so their overlap is negligible, and hence the normalization $P_1 = \int dx_1 |\psi_1(x_1, z_1 = 0)|^2 = 1$ is satisfied.

To calculate the perturbative function $\frac{\delta}{\delta\chi(x)}P_{3bo}$, we first substitute this into Eq.(21) to calculate the two functions $\phi_b(x)$, $\psi_{2a}(x)$, we get

$$\begin{aligned}\frac{\delta}{\delta\chi(x)}P_{3bo} &= \phi_b(x)\psi_{2a}(x) + c.c. \\ \psi_{2a}(x) &\equiv \int dx_1 G(x, x_1; t)\psi_1(x_1) = \frac{1}{\sqrt{2}} \int dx_1 G(x, x_1; t) (\psi_{1+}(x_1) + \psi_{1-}(x_1)) \equiv \frac{1}{\sqrt{2}} (\psi_{2a+}(x) + \psi_{2a-}(x)) \\ \psi_{2b+}(x_2) &= f_2(x_2) \int dx_1 G(x_2, x_1; t_1, 0)\psi_{1+}(x_1) \\ \psi_{2b-}(x_2) &= f_2(x_2) \int dx_1 G(x_2, x_1; t_1, 0)\psi_{1-}(x_1) \\ \phi_b(x) &\equiv \int dx_2 (\psi_{2b}^*(x_2, t_1) f_2(x_2) G(x_2, x; t_L - t)) \\ &\equiv \frac{1}{\sqrt{2}} \int dx_2 \{ (\psi_{2b+}^*(x_2, t_1) + \psi_{2b-}^*(x_2, t_1)) f_2(x_2) G(x_2, x; t_L - t) \} \equiv \frac{1}{\sqrt{2}} (\phi_{b+}(x) + \phi_{b-}(x))\end{aligned}\quad (42)$$

We can obtain each of the four terms $\psi_{2a+}(x)$, $\psi_{2a-}(x)$, $\phi_{b+}(x)$, $\phi_{b-}(x)$ in a more explicit form by replacing s_1 by either s_1 or $-s_1$ in the expression of $\phi_b(x)$ of Eq.(28) and separately the expression of $\psi_{2a}(x)$ of Eq.(29). Then we get the perturbative function between the entrance and the slit 3

$$\begin{aligned}\frac{\delta}{\delta\chi(x)}P_{3bo} &= \frac{(\phi_{b+}(x) + \phi_{b-}(x)) (\psi_{2a+}(x) + \psi_{2a-}(x))}{\sqrt{2}} + c.c. \\ &= \frac{1}{2} (\phi_{b+}(x)\psi_{2a+}(x) + \phi_{b-}(x)\psi_{2a-}(x) + \phi_{b+}(x)\psi_{2a-}(x) + \phi_{b-}(x)\psi_{2a+}(x) + c.c.)\end{aligned}\quad (43)$$

So the interference pattern $P_{3bo}(s_3)$ is obtained by the integration in Eq.(23), using the Gaussian integral Eq.(9)

$$\begin{aligned}P_{3bo} &= \frac{1}{2} \int_{-\infty}^{\infty} dx \frac{\delta}{\delta\chi(x)}P_{3bo} = \int_{-\infty}^{\infty} dq \frac{1}{4} (\phi_{b+}(x)\psi_{2a+}(x) + \phi_{b-}(x)\psi_{2a-}(x) + \phi_{b+}(x)\psi_{2a-}(x) + \phi_{b-}(x)\psi_{2a+}(x) + c.c.) \\ &= \int_{-\infty}^{\infty} dq \frac{1}{2} \text{Re} (\phi_{b+}(x)\psi_{2a+}(x) + \phi_{b-}(x)\psi_{2a-}(x) + \phi_{b+}(x)\psi_{2a-}(x) + \phi_{b-}(x)\psi_{2a+}(x))\end{aligned}\quad (44)$$

For the same set of parameters as in Fig. 2, i.e., photon wavelength $\lambda = 0.5\mu m$, $z_3 = 2m$, $\sigma_1 = 50\mu m$, $\sigma_3 = 4\mu m$ except that $s_1 = 0$ is replaced by $\pm s_1 = \pm 1mm$ for the double slit experiment, Fig. 4(a) shows $P_{3bo}(s_3) = \frac{1}{2} \int_{-\infty}^{\infty} dx \frac{\delta P_{3bo}}{\delta f_2(x,z)}$ calculated at $z = 1.9m$. However, as discussed above, the plot is independent of z : it is the same for any $0 < z < 2m$. In Fig.4(b), we choose $s_3 = 0$, where $P_{3bo} = 0.004122$ reaches the peak. To verify this result, we use the method in Eq.(18) to directly calculate $P_{3bo} = 0.002061$ with only one of the slits open. So the interference peak is twice the probability of a single slit. It is only twice, not 4 times because the normalization of $\psi_1(x_1)$ requires that it is reduced by $\sqrt{2}$ in Eq.(41). For this peak point shown as the red dot in Fig. 4(a), the perturbative function $\frac{\delta}{\delta f_2(x)} P_{3bo}$ waveform is shown in Fig. 4(b). There are two spindle-shaped regions symmetrically oriented where $\frac{\delta}{\delta f_2(x_2)} P_{3b} > 0$ varies slowly, and both have a color between yellow to deep red and are in phase. In Fig. 4(c), we choose $s_3 = -0.25mm$, where $P_{3bo} = \frac{1}{2} \int_{-\infty}^{\infty} dx \frac{\delta P_{3bo}}{\delta f_2(x,z)} = 1.249 \times 10^{-5}$ reaches the minimum shown in Fig. 4(a) as the green dot; the two spindle-shaped regions have different colors. In the upper plane, the region is colored red. The lower region is colored blue, with a phase difference of π . Because of the finite size of σ_3 , the minimum $P_{3bo} = 1.249 \times 10^{-5}$ is not zero. In this case, the positive peaks of $\frac{\delta P_{3bo}}{\delta f_2(x,z)}$ in the integration $P_{3bo} = \frac{1}{2} \int_{-\infty}^{\infty} dx \frac{\delta P_{3bo}}{\delta f_2(x,z)}$ almost cancel the negative peaks over the $x - z$ plane. Notice that even though $\frac{\delta P_{3bo}}{\delta f_2(x,z)}$ depends on z , the integral is independent of z . This independence further confirms what we emphasized in Section 4.2 about Eq.(23) that the probability P_{3bo} is already determined right in the beginning at the entrance slit 1 with $z = 0_+$, even though it is measured at the exit slit after the wave packet (the particle) passes through the whole system.

6. SUMMARY

We study the wave packet evolution when a single particle travels in the free space between two slits before it arrives at the detector behind the exit slit. We use a narrow pin to perturbatively block the wave function in repeated experiments to count the detection rate as a function of the pin's transverse and longitudinal position (x, z) .

When we normalize the probability of entering the entrance slit as 1, the perturbative function $\frac{\delta P_{3bo}}{\delta f_2(x,z)}$ measured this way is the functional derivative of the probability P_{3bo} of detection. The result shows this function is a real-valued function with phase information. The shape of the function is very different from the well-known solution $\psi_{2a}(x, z)$ of the Schrödinger equation with the given initial wave function $\psi_1(x_1, z_1)$. This perturbative function $\frac{\delta P_{3bo}}{\delta f_2(x,z)}$ forms a spindle-shaped region between the two slits with two pointed ends positioned at the two slits, while $|\psi_{2a}(x, z)|^2$ forms a fan-shaped region with only the pointed end at the entrance slit. While we determine $\psi_{2a}(x, z)$ by specifying the initial value of s_1 only, the perturbative function $\frac{\delta P_{3bo}}{\delta f_2(x,z)}$ is determined by both the initial s_1 and final s_3 , somewhat like in the classical theory, where we determine the particle trajectory by two points, i.e., the initial and final position. While $|\psi_{2a}(x, z)|^2$ provides a statistical distribution of final states, the perturbative function $\frac{\delta P_{3bo}}{\delta f_2(x,z)}$ provides a specific, definite, completely reproducible result once s_3 is set up in an experiment.

The integral $\frac{1}{2} \int_{-\infty}^{\infty} dx \frac{\delta P_{3bo}}{\delta f_2(x,z)}$ at any given z between the two slits provides the detection probability P_{3bo} no matter where z is, even for $z = 0_+$, i.e., right at the beginning. This result shows the probability of detection at a given point s_3 is determined long before the particle arrives at the detector. This outcome, in turn, means that once the experiment confirms the prediction of $\frac{\delta P_{3bo}}{\delta f_2(x,z)}$, it provides a picture of the wave packet evolution different from that of a cylindrical wavefront of propagation that starts from the source slit and then continues to widespread at the exit slit. The picture provided by $\frac{\delta P_{3bo}}{\delta f_2(x,z)}$ is that the source emits spindle-shaped wave packets into various directions to arrive at different detectors at various positions indexed as s_{3n} , each with a probability $P_{3bo}(s_{3n})$. If the width σ_3 of slit 3 is sufficiently small, in a hypothetical experiment, a set of slits s_{3n} spaced by $\sqrt{2}\pi\sigma_3$ extending over the exit screen would have a combined detection probability of one for a set of idealized detectors with 100% quantum efficiency. This probability of one means the probability amplitude $\psi_{2a}(x, z)$ represents the distribution of an ensemble of single-particle wave packets. While $\frac{\delta P_{3bo}}{\delta f_2(x,z)}$ represents one specific state in the ensemble. Thus, one can separate the wave function collapse process into two: First, from the ensemble of states, one state is sampled; second, in the specific sampled state, the particle wavepacket evolves according to the function $\frac{\delta P_{3bo}}{\delta f_2(x,z)}$ starting from the source point, growing to a maximum in the middle of the slit 1 and 3, then converging to the exit slit 3. The first step is more like a conceptual change of our knowledge from uncertainty to certainty rather than a continuous process like the one in the second step, where a wave packet collapses into a point embodied as a particle.

We find the explicit expression $\frac{\delta P_{3bo}}{\delta \chi(x)} = P_{3bo} \frac{\sqrt{-\alpha_\chi}}{\sqrt{\pi}} \exp(\alpha_\chi (x - x_c)^2) + c.c.$, and we derive the expression for P_{3bo}, α_χ , and x_c . Then, from these, we calculated the maximum phase π shift width x_π , and the envelope width σ_w of the spindle-shaped function $\frac{\delta P_{3bo}}{\delta \chi(x)}$, and we also used the Poisson distribution formula to calculate the RMS error of the counting measurement of $\frac{\delta P_{3bo}}{\delta \chi(x)}$ as $\frac{1}{\sqrt{n}}$ which is to be used to check against the experiment. In section 4.6, the estimate shows the experiment is feasible.

One might have a few questions. First, why in the very beginning, right after passing the slit 1, the probability is already determined long before the particles arrive at the exit slit. However, this does not violate the causality because the initial wave function $\psi_1(x_1, z_1)$ only gives a distribution of states based on the Born rule, and the final result with probability P_{3bo} is only one state in the distribution.

Second, another question arises when we notice that the function $\frac{\delta P_{3bo}}{\delta \chi(x, z=0_+)}$ depends on $z_3 = L$, so if in a thought experiment, we move the end slit longitudinally to a different L after the particle has passed the entrance slit, in principle the function $\frac{\delta P_{3bo}}{\delta \chi(x, z=0_+)}$ would have changed too even before the particle arrives at the exit slit. The question would be how the position change of the detector at the end can influence the function $\frac{\delta P_{3bo}}{\delta \chi(x, z=0_+)}$ determined at the beginning. However, this also does not violate causality because the wave function evolution is determined by the unitary transform given by the Schrödinger equation and because of the time-reverse symmetry of the equation. We may consider the set $\{s_{3n}\}$ of the detectors arranged to extend over the exit screen we mentioned before. When finally the particle is detected at s_{3n} , its state can only be a δ -function at s_{3n} , initially, the perturbative function must be $\frac{\delta P_{3bo}(s_{3n})}{\delta \chi(x, z=0_+)}$ because only the state represented by $\frac{\delta P_{3bo}(s_{3n})}{\delta \chi(x, z=0_+)}$ can evolve into the point s_{3n} at the detector. When we prepare the initial state as $\psi_1(x_1, z_1)$ by sending particles into the entrance slit, it must have immediately become a distribution if we set up the set of detectors $\{s_{3n}\}$ at $t_3 = \frac{z_3}{v}$.

In the Heisenberg picture, this becomes clearer, as we discussed in Appendix I. We denote the initial position operator in the Heisenberg picture as $X_H(t_1) = X_S$ because it is the same as in the Schrödinger picture. We denote the position operator at time t_3 as $X_H(t_3)$ and denote the evolution operator from t_1 to t_3 as $U(t_3)$, then $X_H(t_3) = U^\dagger X_S U$. We denote the eigenstate of $X(t_3)$ as $u_{x_3}(x_0)$, i.e., $X(t_3)u_{x_3}(x_0) = x_3 u_{x_3}(x_0)$. Because a state vector in the Heisenberg picture does not change with time, the state $u_{x_3}(x_0)$ is also the initial state vector in the Schrödinger picture. In the Schrödinger picture, the state $u_{x_3}(x_0)$ will evolve into the eigenvector $U(t_3)u_{x_3}(x_0)$, and this must be the eigenstate of the X_S , i.e., $X_S U(t_3)u_{x_3}(x_0) = x_3 U(t_3)u_{x_3}(x_0)$. Hence, $U(t_3)u_{x_3}(x_0)$ is the δ -function at x_3 . In other words, $u_{x_3}(x_0)$ is the initial wave function that eventually evolves into the eigenstate of position operator X_S in the Schrödinger picture at position x_3 . If the detector at s_{3n} detects the particle, then $x_3 = s_{3n}$.

The complete orthonormal basis $\{u_{x_3}(x_0)\}$ in the Schrödinger picture will evolve into the complete basis consisting of δ -functions at $\{x_3\}$. Thus, the initial state can only be one in this set of functions $\{u_{x_3}(x_0)\}$ as long as we set the detectors at position $z_3 = L$. This set of functions depends on L . If we change L , the set $\{u_{x_3}(x_0)\}$ will change too. There is no causality violation here because the unitary transform by the evolution operator $U(t_3)$ determines this relation between the position of detectors and $\{u_{x_3}(x_0)\}$. We assume the wave function is a linear combination of δ -functions at time t_3 , and the probability distribution follows the Born rule. When we apply the unitary transform U^{-1} to this final distribution of δ -functions to derive the initial function, the result must be the linear combination of $\{u_{x_3}(x_0)\}$, and the probability distribution must follow the Born rule. This conclusion means the initial state cannot be a δ -function; it has to be a distribution of $\{u_{x_3}(x_0)\}$. If the experiment prepares a δ -function as the initial state, it would immediately become a distribution of $\{u_{x_3}(x_0)\}$ according to the Born rule. It is just like if we view an object from different perspectives, we will reveal other aspects of the object. According to the uncertainty principle, we also reach the same conclusion: $X_H(t_1)$ and $X_H(t_3) = X_S + \frac{P_S}{M}(t_3 - t_1)$ do not commute; they cannot have the same eigenvector. When the detector s_{3n} detects a particle, its state vector is an eigenstate of $X_H(t_3)$; hence, its initial state cannot be an eigenstate of $X_H(t_1)$. Even though we prepare an eigenstate of the initial $X_H(t_1)$, it is already a distribution of $\{u_{x_3}(x_0)\}$ the moment we prepare it because the detector array is not at the origin at slit 1.

We proposed and analyzed the basic principle of an experiment using photons at a wavelength of $0.5\mu m$. Many aspects of the problem need to be studied further. For example, it would be interesting to study the feasibility of other wavelengths or particles. It would also be interesting to study the effect of the photon's finite bandwidth and pulse length and see if it will affect the width of the spindle-shaped region.

We thank Professor C. N. Yang for drawing our attention to the problem of dissipative systems, for spending his valuable time in many sessions of stimulating discussions on this subject, and for many suggestions that are critically important for work on the dissipative systems [12], which finally leads to the topics in the present work. We thank Dr. T. Shaftan, Dr. V. Smaluk for their discussion and suggestions on the manuscript.

APPENDIX I DERIVE GREEN'S FUNCTION $G(x_1, x_0; t)$ IN HEISENBERG PICTURE

We derive Green's function $G(x_1, x_0; t)$ in the Heisenberg Picture using the method used in our work on dissipative systems [12]. Instead of using x_1, t_1, x_3, t_3 as position and time at slits 1 and 2 as in Fig. 1, we use initial position and time $x_0, 0$ and x, t to avoid confusing the derivation with the derivation elsewhere, so that when we apply the Green's function, we replace the indices. We write

$$x(t) = x_0 + \frac{p_0}{M}t = x_0 - t \frac{i\hbar}{M} \frac{\partial}{\partial x_0} \quad (45)$$

The eigenfunction of $x(t)$ with an eigenvalue denoted by x_1 , in the x_0 representation, is easily calculated to be

$$u_{x_1}(x_0, t) = \left(\frac{M}{2\pi\hbar t} \right)^{\frac{1}{2}} \exp \left[-i \frac{M}{2\hbar t} (x_0^2 - 2x_1x_0 + \phi(x_1, t)) \right], \quad (46)$$

with ϕ as an arbitrary phase, i.e., a real number. This eigenfunction is related to Green's function $G(x_1, x_0; t) = \langle x_1 | U(t) | x_0 \rangle$ where $U(t)$ is the evolution operator. To see this, we use the relation between the Schoedinger operator \mathbf{X}_S and the Heisenberg operator $X(t) \equiv \mathbf{X}_H(t) = U^{-1}(t)\mathbf{X}_S U(t)$.

Let $|x_1\rangle$ be the eigenvector of \mathbf{X}_S with eigenvalue x_1 , i.e.,

$$\mathbf{X}_S |x_1\rangle = x_1 |x_1\rangle \quad (47)$$

we see that $U^{-1}|x_1\rangle$ is the eigenvector of $X(t)$ of value x_1

$$X(t)U^{-1}|x_1\rangle = \mathbf{X}_H U^{-1}|x_1\rangle = U^{-1}\mathbf{X}_S U U^{-1}|x_1\rangle = U^{-1}\mathbf{X}_S |x_1\rangle = x_1 U^{-1}|x_1\rangle \quad (48)$$

So $U^{-1}|x_1\rangle$ is the eigenvector of $X(t)$, thus it is proportional to $u_{x_1}(x_0, t)$. We have $u_{x_1}(x_0, t) = \langle x_0 | U^{-1}(t) | x_1 \rangle = \langle x_0 | U^\dagger(t) | x_1 \rangle = G^*(x_1, x_0; t)$, where the evolution operator by $U(t)$ is unitary when we choose the eigenvectors of $x(t)$ to be orthonormal. Thus we have

$$G(x_1, x_0; t) = u_{x_1}^*(x_0, t) = \left(\frac{M}{2\pi\hbar t} \right)^{\frac{1}{2}} \exp \left[i \frac{M}{2\hbar t} (x_0^2 - 2x_1x_0 + \phi(x_1, t)) \right] \quad (49)$$

Next, we shall determine the arbitrary phase $\phi(x_1, t)$, the phase of the eigenvectors of $x(t)$ in Eq. (46). Since p is constant in free space, $p(t) = p_0$

The eigenfunction of $p(t)$ can be calculated in two ways. (a) We can calculate the eigenvector of $p(t) = p_0 = -\frac{i\hbar}{M} \frac{\partial}{\partial x_0}$ in the x_0 representation and then use the Green's function Eq. (49) to transform it into the $x(t)$ representation. (b) The eigenfunction of $p(t)$ with eigenvalue p_1 is $e^{i\frac{p_1}{\hbar}x_1}$. By comparing these two solutions, the arbitrary phase $\phi(x_1, t)$ in the Green's function is determined to be within a phase $\phi(t)$, which is independent of x_1 . $\phi(t)$ is an arbitrary real function of time, except that $\phi(0) = 0$ so that it satisfies the condition that at $t = 0$, the Green's function becomes $\delta(x_1 - x_0)$.

$$G(x_1, x_0; t) = \left(\frac{M}{2\pi i \hbar t} \right)^{\frac{1}{2}} \exp \left[i \frac{M}{2\hbar t} (x_0^2 - 2x_1 x_0 + x_1^2) - \frac{i}{\hbar} \phi(t) \right] \quad (50)$$

When substituting $G(x_1, x_0; t)$ into the Schrödinger equation (4), it requires $\dot{\phi}(t) = 0$. Since $\phi(0) = 0$, $\phi(t) = 0$. Thus we obtain the Green's function:

$$G(x_1, x_0; t) = \left(\frac{M}{2\pi i \hbar t} \right)^{\frac{1}{2}} \exp \left[i \frac{M}{2\hbar t} (x_1 - x_0)^2 \right] \quad (51)$$

APPENDIX II WAVE FUNCTION PROPAGATION FROM SLIT 1 TO SLIT 3

II.1 Propagation formula and slit formula With $\alpha_1 = -\frac{1}{4\sigma_1^2}$, $c_1 = \frac{1}{4} \ln \left(\frac{1}{2\pi\sigma_1^2} \right)$, $\beta_1 = \frac{1}{4d_1}$, $d_1 = \frac{\hbar t}{2M} = \frac{\lambda z}{4\pi}$, $\alpha_{f2} = -\frac{1}{4\sigma_2^2}$ in Eq.(8,11), we have

Propagation formula Eq.(10),

$$\begin{aligned} \ln \psi_{2a}(x_2, t) &= \alpha_{2a} (x_2 - s_2)^2 + c_{2a} \\ \alpha_{2a} &= \frac{i\alpha_1\beta_1}{(\alpha_1 + i\beta_1)} = \frac{1}{\frac{1}{\alpha_1} - i\frac{1}{\beta_1}} \\ s_{2a} &= s_1 \\ c_{2a} &= \frac{1}{2} \ln \left(\frac{\alpha_{2a}}{\alpha_1} \right) + c_1 \end{aligned} \quad (52)$$

Slit formula Eq.(11),

$$\begin{aligned} \ln \psi_{2b}(x_2, z_2 = z) &= \alpha_{2b} (x_2 - s_{2b})^2 + c_{2b} \\ \alpha_{2b} &= \alpha_{2a} + \alpha_{f2} \\ s_{2b} &= \frac{\alpha_{2a}s_{2a} + \alpha_{f2}s_2}{\alpha_{2a} + \alpha_{f2}} \\ c_{2b} &= -\alpha_{2b}s_{2b}^2 + \alpha_{2a}s_{2a}^2 + \alpha_{f2}s_2^2 + c_{2a} \end{aligned} \quad (53)$$

II.2 α pattern, We find a pattern for propagation followed by slit as follows.

Apply the two formulas of II.1, we find,

$$\begin{aligned} \frac{1}{\alpha_{2a}} &= \frac{1}{\alpha_1} - i\frac{1}{\beta_1} \\ \alpha_{2b} &= \alpha_{2a} + \alpha_{f2} \\ \frac{1}{\alpha_{3a}} &= \frac{1}{\alpha_{2b}} - i\frac{1}{\beta_2} \\ \alpha_{3b} &= \alpha_{3a} + \alpha_{f3} \end{aligned} \quad (54)$$

with $\beta_2 = \frac{1}{4d_2}$, $d_2 = \frac{\lambda(L-z)}{4\pi}$.

We introduce Δ_1, Δ_2 when following steps in Eq.(54) to find a pattern for the expression of α 's

$$\Delta_1 \equiv \sigma_1^2 + id_1, \Delta_2 \equiv \sigma_2^2 \frac{\Delta_1}{\Delta_1 + \sigma_2^2} + id_2 \quad (55)$$

$$\begin{aligned} \frac{1}{\alpha_{2a}} &= -4(\sigma_1^2 + id_1) \equiv -4\Delta_1, \alpha_{2b} = \alpha_{2a} + \alpha_{f2} = -\frac{1}{4\Delta_1} - \frac{1}{4\sigma_2^2} \\ \frac{1}{\alpha_{2b}} &= -\frac{1}{\frac{1}{4\Delta_1} + \frac{1}{4\sigma_2^2}} = -4\sigma_2^2 \frac{\Delta_1}{\sigma_2^2 + \Delta_1} \\ \frac{1}{\alpha_{3a}} &= \frac{1}{\alpha_{2b}} - i\frac{1}{\beta_2} = -4\sigma_2^2 \frac{\Delta_1}{\sigma_2^2 + \Delta_1} - i4d_2 = -4\left(\sigma_2^2 \frac{\Delta_1}{\sigma_2^2 + \Delta_1} + id_2\right) \equiv -4\Delta_2 \\ \alpha_{3b} &= \alpha_{3a} + \alpha_{f2} = -\frac{1}{4\Delta_2} - \frac{1}{4\sigma_3^2}, \frac{1}{\alpha_{3b}} = -\frac{1}{\frac{1}{4\Delta_2} + \frac{1}{4\sigma_3^2}} = -4\sigma_3^2 \frac{\Delta_2}{\Delta_2 + \sigma_3^2} \end{aligned} \quad (56)$$

The α pattern is

$$\begin{aligned} \frac{1}{\alpha_1} &= -4\sigma_1^2 \\ \frac{1}{\alpha_{2a}} &= -4\Delta_1, \frac{1}{\alpha_{2b}} = -4\sigma_2^2 \frac{\Delta_1}{\Delta_1 + \sigma_2^2} \\ \frac{1}{\alpha_{3a}} &= -4\Delta_2, \frac{1}{\alpha_{3b}} = -4\sigma_3^2 \frac{\Delta_2}{\Delta_2 + \sigma_3^2} \end{aligned} \quad (57)$$

II.3 s pattern Following the pattern section II.2, we look for similar pattern for $s_{2a}, s_{2b}, s_{3a}, s_{3b}$.

Follow Eq.(13), and use α -pattern of I.2, we derive in the following steps

$$\begin{aligned} s_{2a} &= s_1 \\ s_{2b} &= \frac{\alpha_{2a}s_{2a} + \alpha_{f2}s_2}{\alpha_{2a} + \alpha_{f2}} = \frac{\left(\frac{s_{2a}}{\alpha_{f2}} + \frac{s_2}{\alpha_{2a}}\right)}{\left(\frac{1}{\alpha_{2a}} + \frac{1}{\alpha_{f2}}\right)} = \frac{-4\sigma_2^2 s_{2a} - 4\Delta_1 s_2}{(-4\Delta_1 - 4\sigma_2^2)} = \frac{\sigma_2^2 s_{2a} + \Delta_1 s_2}{\Delta_1 + \sigma_2^2} \\ &= \frac{\sigma_2^2 s_1 + \Delta_1 s_2}{\Delta_1 + \sigma_2^2} = s_2 \frac{\Delta_1}{\Delta_1 + \sigma_2^2} + \frac{\Delta_1 s_1 + \sigma_2^2 s_1 - \Delta_1 s_1}{\Delta_1 + \sigma_2^2} \\ &= (s_2 - s_1) \frac{\Delta_1}{\Delta_1 + \sigma_2^2} + s_1 \\ s_{3a} &= s_{2b} \\ s_{3b} &= \frac{(\alpha_{3a}s_{3a} + \alpha_{f3}s_3)}{(\alpha_{3a} + \alpha_{f3})} = \frac{\left(\frac{1}{-4\Delta_2} s_{2b} - \frac{1}{4\sigma_3^2} s_3\right)}{\left(\frac{1}{-4\Delta_2} - \frac{1}{4\sigma_3^2}\right)} = \frac{(\sigma_3^2 s_{2b} + \Delta_2 s_3)}{(\Delta_2 + \sigma_3^2)} \end{aligned} \quad (58)$$

following the pattern above of s_{2b}

$$s_{3b} = (s_3 - s_{2b}) \frac{\Delta_2}{\Delta_2 + \sigma_3^2} + s_{2b}$$

Thus we have a pattern up to s_{3b}

$$\begin{aligned}
s_{2a} &= s_1 \\
s_{2b} &= (s_2 - s_1) \frac{\Delta_1}{\Delta_1 + \sigma_2^2} + s_1 \\
s_{3a} &= s_{2b} \\
s_{3b} &= (s_3 - s_{2b}) \frac{\Delta_2}{\Delta_2 + \sigma_3^2} + s_{2b}
\end{aligned} \tag{59}$$

II.4 c pattern, following the following steps, we have a list for $c_1, c_{2a}, \dots, c_{3b}$, Using Eq.(57) and Eq.(11,58,59), we use the following steps to find explicit expressions for c_{2b} ,

$$\begin{aligned}
c_{2b} &= -\alpha_{2b}s_{2b}^2 + \alpha_{2a}s_{2a}^2 + \alpha_{f2}s_2^2 + c_{2a} \\
\alpha_{2a} &= -\frac{1}{4\Delta_1}, \alpha_{2b} = -\frac{1}{4\Delta_1} \frac{\Delta_1 + \sigma_2^2}{\sigma_2^2}, \alpha_{f2} = -\frac{1}{4\sigma_2^2} \\
c_{2b} &= \frac{1}{4\Delta_1} \frac{\Delta_1 + \sigma_2^2}{\sigma_1^2} s_{2b}^2 - \frac{1}{4\Delta_1} s_{2a}^2 - \frac{1}{4\sigma_2^2} s_2^2 + c_{2a} \\
s_{2b} &= \frac{\sigma_2^2 s_{2a} + \Delta_1 s_2}{\Delta_1 + \sigma_2^2}, s_{2a} = s_1 \\
c_{2b} &= -\frac{s_2^2}{4\sigma_2^2} - \frac{s_1^2}{4\Delta_1} + \frac{(\Delta_1 s_2 + s_1 \sigma_2^2)^2}{4\Delta_1 \sigma_2^2 (\Delta_1 + \sigma_2^2)} + c_{2a} = -\frac{(s_1 - s_2)^2}{4\Delta_1 + 4\sigma_2^2} + c_{2a}
\end{aligned} \tag{60}$$

Continue this way leads to a c -pattern,

$$\begin{aligned}
c_1 &= \frac{1}{4} \ln \left(\frac{1}{2\pi\sigma_1^2} \right), c_{2a} = \frac{1}{2} \ln \left(\frac{\alpha_{2a}}{\alpha_1} \right) + c_1 = \frac{1}{2} \ln \left(\frac{\sigma_1^2}{\Delta_1} \right) + \frac{1}{4} \ln \left(\frac{1}{2\pi\sigma_1^2} \right) \\
c_{2b} &= -\frac{(s_1 - s_2)^2}{4(\Delta_1 + \sigma_2^2)} + c_{2a} = -\frac{(s_1 - s_2)^2}{4(\Delta_1 + \sigma_2^2)} + \frac{1}{2} \ln \left(\frac{\sigma_1^2}{\Delta_1} \right) + \frac{1}{4} \ln \left(\frac{1}{2\pi\sigma_1^2} \right) \\
c_{3a} &= \frac{1}{2} \ln \left(\frac{\alpha_{3a}}{\alpha_{2b}} \right) + c_{2b} = -\frac{(s_1 - s_2)^2}{4(\Delta_1 + \sigma_2^2)} + \frac{1}{2} \ln \left(\frac{\sigma_2^2}{\Delta_1 + \sigma_2^2} \frac{\sigma_1^2}{\Delta_2} \right) + \frac{1}{4} \ln \left(\frac{1}{2\pi\sigma_1^2} \right) \\
c_{3b} &= -\frac{(s_3 - s_{2b})^2}{4(\Delta_2 + \sigma_3^2)} - \frac{(s_1 - s_2)^2}{4(\Delta_1 + \sigma_2^2)} + \frac{1}{2} \ln \left(\frac{\sigma_2^2}{\Delta_1 + \sigma_2^2} \frac{\sigma_1^2}{\Delta_2} \right) + \frac{1}{4} \ln \left(\frac{1}{2\pi\sigma_1^2} \right)
\end{aligned} \tag{61}$$

II.5 ψ -pattern All the steps above applied to Eq.(7) lead to the ψ -pattern finally,

$$\begin{aligned}
\ln \psi_1(x_1, 0) &= \alpha_1(x_1 - s_1)^2 + c_1 = -\frac{1}{4\sigma_1^2}(x_1 - s_1)^2 + \frac{1}{4} \ln \left(\frac{1}{2\pi\sigma_1^2} \right) \\
\ln \psi_{2a}(x_2, t_1) &= \alpha_{2a}(x_2 - s_{2a})^2 + c_{2a} = -\frac{1}{4\Delta_1}(x_2 - s_1)^2 + \frac{1}{2} \ln \left(\frac{\sigma_1^2}{\Delta_1} \right) + \frac{1}{4} \ln \left(\frac{1}{2\pi\sigma_1^2} \right) \\
\ln \psi_{2b}(x_2, t_1) &= \alpha_{2b}(x_2 - s_{2b})^2 + c_{2b} = -\frac{1}{4\Delta_1} \frac{\Delta_1 + \sigma_2^2}{\sigma_2^2} (x_2 - s_{2b})^2 - \frac{(s_1 - s_2)^2}{4(\Delta_1 + \sigma_2^2)} + \frac{1}{2} \ln \left(\frac{\sigma_1^2}{\Delta_1} \right) + \frac{1}{4} \ln \left(\frac{1}{2\pi\sigma_1^2} \right) \\
\ln \psi_{3a}(x_3, t_2 + t_1) &= \alpha_{3a}(x_3 - s_{3a})^2 + c_{3a} = -\frac{1}{4\Delta_2}(x_3 - s_{2b})^2 - \frac{(s_1 - s_2)^2}{4(\Delta_1 + \sigma_2^2)} + \frac{1}{2} \ln \left(\frac{\sigma_2^2}{\Delta_1 + \sigma_2^2} \frac{\sigma_1^2}{\Delta_2} \right) + \frac{1}{4} \ln \left(\frac{1}{2\pi\sigma_1^2} \right) \\
\ln \psi_{3b}(x_3, t_2 + t_1) &= \alpha_{3b}(x_3 - s_{3b})^2 + c_{3b} \\
&= -\frac{1}{4\Delta_2} \frac{\Delta_2 + \sigma_3^2}{\sigma_3^2} (x_3 - s_{3b})^2 - \frac{(s_3 - s_{2b})^2}{4(\Delta_2 + \sigma_3^2)} - \frac{(s_1 - s_2)^2}{4(\Delta_1 + \sigma_2^2)} + \frac{1}{2} \ln \left(\frac{\sigma_2^2}{\Delta_1 + \sigma_2^2} \frac{\sigma_1^2}{\Delta_2} \right) + \frac{1}{4} \ln \left(\frac{1}{2\pi\sigma_1^2} \right)
\end{aligned} \tag{62}$$

where,

$$\begin{aligned}
s_{2b} &= (s_2 - s_1) \frac{\Delta_1}{\Delta_1 + \sigma_2^2} + s_1 \\
s_{3b} &= (s_3 - s_{2b}) \frac{\Delta_2}{\Delta_2 + \sigma_3^2} + s_{2b} \\
\Delta_1 &\equiv \sigma_1^2 + id_1, \beta_1 = \frac{1}{4d_1}, d_1 = \frac{\hbar t}{2M} = \frac{\lambda z}{4\pi} \\
\Delta_2 &\equiv \sigma_2^2 \frac{\Delta_1}{\Delta_1 + \sigma_2^2} + id_2, \beta_2 = \frac{1}{4d_2}, d_2 = \frac{\hbar(t_3 - t_2)}{2M} = \frac{\lambda(L - z)}{4\pi}
\end{aligned} \tag{63}$$

APPENDIX III SIMPLIFIED ANALYTICAL EXPRESSION OF P_{2b}

The P_{2b} expression of Section 3.1 is analytical but expressed by $\alpha_{2b}, s_{2b}, c_{2b}$ that in turn are represented by $\alpha_{2a}, s_{2a}, c_{2a}$, not by the parameters directly used in the experiment,

$$P_{2b}(s_2, \sigma_2, z_2) = \sqrt{\frac{\pi}{-2\text{Re}(\alpha_{2b})}} \exp \left(-2 \frac{|\alpha_{2b}|^2 (\text{Im}(s_{2b}))^2}{\text{Re}(\alpha_{2b})} + 2\text{Re}(c_{2b}) \right) \tag{64}$$

When we express it using these direct parameters by a series of substitutions, it becomes a long and complicated expression that needs to be simplified. We shall outline some intermediate steps to avoid writing down tedious derivation and cluttering. First, we substitute c_{2b} from Eq.(13), and simplify the real and imaginary parts of the results in terms of two scaled dimensionless parameters, μ, ρ

$$\begin{aligned}
P_{2b} &= \sqrt{\frac{\pi}{-2\text{Re}(\alpha_{2b})}} \exp\left(\frac{|\alpha_{2b}|^2 (s_{2b} - s_{2b}^*)^2}{2\text{Re}(\alpha_{2b})} + 2\text{Re}\left(-\frac{(s_1 - s_2)^2}{4(\Delta_1 + \sigma_2^2)} + \frac{1}{2} \ln\left(\frac{\sigma_1^2}{\Delta_1}\right) + \frac{1}{4} \ln\left(\frac{1}{2\pi\sigma_1^2}\right)\right)\right) \\
\mu &\equiv \frac{\sigma_1^2}{d_1}, \rho \equiv \frac{\sigma_2^2}{\sigma_1^2} \\
\text{Re}(\alpha_{2b}) &= \frac{1}{2} \left(-\frac{1}{4\sigma_2^2} \frac{\Delta_1 + \sigma_2^2}{\Delta_1} - \frac{1}{4\sigma_2^2} \frac{\Delta_1^* + \sigma_2^2}{\Delta_1^*}\right) = -\frac{1}{4\sigma_2^2} \frac{\sigma_1^4 + d_1^2 + \sigma_1^2\sigma_2^2}{\sigma_1^4 + d_1^2} = -\frac{1}{4\sigma_2^2} \frac{\mu^2 + \rho\mu^2 + 1}{\mu^2 + 1} \\
\exp\left(2\text{Re}\left(\frac{1}{2} \ln\left(\frac{\sigma_1^2}{\Delta_1}\right)\right)\right) &= \exp\left(\frac{1}{2} \ln\left(\frac{\sigma_1^2}{\Delta_1}\right) + \frac{1}{2} \ln\left(\frac{\sigma_1^2}{\Delta_1^*}\right)\right) = \sqrt{\frac{\sigma_1^4}{\sigma_1^4 + d_1^2}} = \sqrt{\frac{\mu^2}{\mu^2 + 1}} \\
\therefore P_{2b} &= \sqrt{\frac{\rho\mu^2}{\mu^2 + \mu^2\rho + 1}} \exp\left(\frac{|\alpha_{2b}|^2 (s_{2b} - s_{2b}^*)^2}{2\text{Re}(\alpha_{2b})} + 2\text{Re}\left(-\frac{(s_1 - s_2)^2}{4(\Delta_1 + \sigma_2^2)}\right)\right)
\end{aligned} \tag{65}$$

We need to simplify $|\alpha_{2b}|^2 (s_{2b} - s_{2b}^*)^2 + 4\text{Re}\left(-\frac{(s_1 - s_2)^2}{4(\Delta_1 + \sigma_2^2)}\right) \text{Re}(\alpha_{2b})$, and we have

$$\begin{aligned}
|\alpha_{2b}|^2 (s_{2b} - s_{2b}^*)^2 &= \frac{1}{16} \frac{1}{\Delta_1 \Delta_1^*} \frac{(\Delta_1 - \Delta_1^*)^2}{(\Delta_1 + \sigma_2^2)(\Delta_1^* + \sigma_2^2)} (s_2 - s_1)^2 \\
4\text{Re}\left(-\frac{(s_1 - s_2)^2}{4(\Delta_1 + \sigma_2^2)}\right) \text{Re}(\alpha_{2b}) &= \frac{1}{16\sigma_2^2} (s_1 - s_2)^2 \left(\frac{\Delta_1 + \sigma_2^2 + \Delta_1^* + \sigma_2^2}{(\Delta_1 + \sigma_2^2)(\Delta_1^* + \sigma_2^2)}\right) \left(\frac{2\Delta_1 \Delta_1^* + \sigma_2^2(\Delta_1 + \Delta_1^*)}{\Delta_1 \Delta_1^*}\right)
\end{aligned}$$

their sum can be simplified, and using $\text{Re}(\alpha_{2b})$ in Eq.(65), we have

$$\begin{aligned}
|\alpha_{2b}|^2 (s_{2b} - s_{2b}^*)^2 + 4\text{Re}\left(-\frac{(s_1 - s_2)^2}{4(\Delta_1 + \sigma_2^2)}\right) \text{Re}(\alpha_{2b}) &= \frac{1}{8\sigma_2^2} (s_1 - s_2)^2 \frac{(\Delta_1 + \Delta_1^*)}{\Delta_1 \Delta_1^*} = \frac{\sigma_1^2}{4\sigma_1^4 \sigma_2^2} \frac{\sigma_1^4}{\sigma_1^4 + d_1^2} (s_1 - s_2)^2 \\
\frac{|\alpha_{2b}|^2 (s_{2b} - s_{2b}^*)^2}{2\text{Re}(\alpha_{2b})} + 2\text{Re}\left(-\frac{(s_1 - s_2)^2}{4(\Delta_1 + \sigma_2^2)}\right) &= \frac{1}{2\text{Re}(\alpha_{2b})} \frac{\sigma_1^2}{4\sigma_1^4 \sigma_2^2} \frac{\sigma_1^4}{\sigma_1^4 + d_1^2} (s_1 - s_2)^2 \\
&= -\frac{1}{2} \frac{4\sigma_2^2 (\sigma_1^4 + d_1^2)}{\sigma_1^4 + d_1^2 + \sigma_1^2 \sigma_2^2} \frac{\sigma_1^2}{4\sigma_1^4 \sigma_2^2} \frac{\sigma_1^4}{\sigma_1^4 + d_1^2} (s_1 - s_2)^2 = -\frac{1}{2} \frac{\sigma_1^2}{\sigma_1^4 + d_1^2 + \sigma_1^2 \sigma_2^2} (s_1 - s_2)^2 = -\frac{1}{2\sigma_1^2} \frac{\mu^2}{\mu^2 + 1 + \rho\mu^2} (s_1 - s_2)^2 \\
\therefore P_{2b} &= \sqrt{\frac{\rho\mu^2}{\mu^2 + \rho\mu^2 + 1}} \exp\left(-\frac{1}{2\sigma_1^2} \frac{\mu^2}{\mu^2 + 1 + \rho\mu^2} (s_1 - s_2)^2\right)
\end{aligned}$$

In the limit of small slit sizes, as $\sigma_1, \sigma_2 \rightarrow 0$, we need to specify their ratio $\rho = \frac{\sigma_2^2}{\sigma_1^2}$, we find

$$P_{2b} = \sqrt{\rho\mu^2} \exp\left(-\frac{\mu^2}{2\sigma_1^2} (s_1 - s_2)^2\right) = \frac{\sigma_1 \sigma_2}{d_1} \exp\left(-\frac{\sigma_1^2}{2d_1^2} (s_1 - s_2)^2\right) \tag{66}$$

APPENDIX IV ANALYTICAL EXPRESSION OF $\frac{\delta P_{3bo}}{\delta \chi(x)} = \phi_b(x) \psi_{2a}(x) + c.c.$

$\frac{\delta P_{3bo}}{\delta \chi(x)}$ and $\frac{\delta P_{3b}}{\delta f_2(x_2)}$ represent the same function with different notation; see Section 4.1

IV.1 Derivation of α_χ

In Section 4.3, Eq.(30), we have

$$\begin{aligned} \ln \phi_b(x)\psi_{2a}(x) &= \alpha_\chi (x - x_c)^2 + C \\ \alpha_\chi &= i\beta_2 - A (i\beta_2)^2 - \frac{1}{4\Delta} \\ A &\equiv \frac{1}{\alpha_{f2} + i\beta_2 + \overline{\alpha_{2b}}} \end{aligned} \quad (67)$$

$\alpha_{f2}, \beta_2, d_2$ are the same as given in section 2.2, $d_1 = \frac{\lambda(z_2 - z_1)}{4\pi} = \frac{\lambda L}{4\pi}$, $d = \frac{\lambda z}{4\pi}$ are given in 4.3. (Notice that the definition of d_1, d_2, d is different from the definition of d_1, d_2, d_L in Section 2.2; this difference is because in the derivation of $\frac{\delta P_{3b0}}{\delta \chi(x)}$ and $\frac{\delta P_{3b}}{\delta f_2(x_2)}$, we replaced the slit 2 in Fig. 1 with a pin and changed notation in Section 4.) Substituting them into α_χ , we have

$$\begin{aligned} \beta_2 &= \frac{M}{2\hbar(t_2 - t)} = \frac{k}{2(L - z)} \equiv \frac{1}{4d_2} = \frac{1}{4(d_1 - d)} \\ \Delta &= \sigma_1^2 + id \\ \overline{\alpha_{2b}} &= -\frac{1}{4\Delta_1} - \frac{1}{4\sigma_2^2} = -\frac{1}{4(\sigma_1^2 - id_1)} - \frac{1}{4\sigma_2^2} = -\frac{\sigma_2^2 + \sigma_1^2 - id_1}{4(\sigma_1^2 - id_1)\sigma_2^2} \\ \frac{1}{A} &= -\frac{1}{4\sigma_2^2} + i\frac{1}{4(d_1 - d)} - \frac{1}{4(\sigma_1^2 - id_1)} - \frac{1}{4\sigma_2^2} = -\frac{1}{4} \left(\frac{2}{\sigma_2^2} - i\frac{1}{(d_1 - d)} + \frac{1}{(\sigma_1^2 - id_1)} \right) \\ \alpha_\chi &= i\frac{1}{4(d_1 - d)} + \frac{\frac{1}{4}\frac{1}{(d_1 - d)}}{-\frac{1}{4} \left(\frac{2}{\sigma_2^2} - i\frac{1}{(d_1 - d)} + \frac{1}{(\sigma_1^2 - id_1)} \right)} - \frac{1}{4(d_1 - d)} - \frac{1}{4(\sigma_1^2 + id)} \end{aligned} \quad (68)$$

After simplification we get

$$\alpha_\chi = \frac{i}{2} \left(\frac{d_1^2 + \sigma_1^4 + \sigma_1^2 \sigma_2^2}{(\sigma_1^2 + id) [2(d_1 - d)(\sigma_1^2 - id_1) - \sigma_2^2(d + i\sigma_1^2)]} \right) \quad (69)$$

Using the dimensionless parameters $\mu \equiv \frac{\sigma_1^2}{d_1}, \rho \equiv \frac{\sigma_2^2}{\sigma_1^2}, \xi \equiv \frac{d}{d_1}$ defined in Eq.(16) and Section 4.3, this becomes

$$\alpha_\chi = -\frac{1}{2\sigma_1^2} \frac{i\mu(\mu^2 + \rho\mu^2 + 1)}{(-i\mu + \xi)(\mu(i\xi - \mu)\rho + 2(\xi - 1)(i\mu + 1))} \quad (70)$$

IV.2 Derivation of x_c

In Section 4.3 Eq.(30) we have

$$x_c = \frac{(Ai\beta_2 (\alpha_{f2}s_2 + \overline{\alpha_{2b}s_{2b}}) - s_1 \frac{1}{4\Delta})}{\alpha_\chi} \quad (71)$$

where $A, \overline{\alpha_{2b}}$, are in Eq.(68), s_{2b} is in Eq.(13), α_{f2} is given in Section 2, substituting these and Eq.(69) for α_χ , we find $x_c = x_{cs1} + x_{cs2}$, each term is linear in s_1, s_2 separately

$$x_{cs1} = -\frac{s_1 (id + \sigma_1^2) (\sigma_2^2 (d + i\sigma_1^2) - 2(-d_1 + d) (id_1 - \sigma_1^2)) (d_1^2 - d_1d + id_1\sigma_1^2 - id\sigma_1^2 + \sigma_1^2\sigma_2^2)}{(d - i\sigma_1^2) (d_1^2 + \sigma_1^4 + \sigma_1^2\sigma_2^2) (2d_1^2 - 2d_1d + 2id_1\sigma_1^2 - 2id\sigma_1^2 - id\sigma_2^2 + \sigma_1^2\sigma_2^2)}$$

$$x_{cs2} = -\frac{s_2 (d_1 + i\sigma_1^2) (id + \sigma_1^2) (\sigma_2^2 (d + i\sigma_1^2) - 2(-d_1 + d) (id_1 - \sigma_1^2))}{(d_1^2 + \sigma_1^4 + \sigma_1^2\sigma_2^2) (2d_1^2 - 2d_1d + 2id_1\sigma_1^2 - 2id\sigma_1^2 - id\sigma_2^2 + \sigma_1^2\sigma_2^2)}$$

The following common factors lead to cancellation

$$2d_1^2 - 2d_1d + 2id_1\sigma_1^2 - 2id\sigma_1^2 - id\sigma_2^2 + \sigma_1^2\sigma_2^2$$

$$= -i (\sigma_2^2 (d + i\sigma_1^2) - 2(-d_1 + d) (id_1 - \sigma_1^2))$$

Finally, we find x_c expressed in terms of the scaled dimensionless parameters μ, ρ in Eq.(16)

$$x_c = \frac{c_{S1}s_1 + c_{S2}s_2}{\mu^2 + \rho\mu^2 + 1}$$

$$c_{S1} \equiv \rho\mu^2 - (i\mu + 1) (\xi - 1)$$

$$c_{S2} \equiv (\mu - i) (\mu + i\xi)$$

-
- [1] Penrose, Roger (May 1996). "On Gravity's role in Quantum State Reduction" (<http://link.springer.com/10.1007/BF02105068>). *General Relativity and Gravitation*. 28 (5): 581–600. doi:10.1007/BF02105068 (<https://doi.org/10.1007%2FBF02105068>). ISSN 0001-7701 (<http://search.worldcat.org/issn/0001-7701>).
- [2] https://en.wikipedia.org/wiki/Wave_function_collapse
- [3] Weinberg, Steven (November 2005). "Einstein's Mistakes". *Physics Today* . 58 (11): 31–35.
- [4] Niels Bohr (1985) [May 16, 1947], Jørgen Kalckar (ed.), Niels Bohr: Collected Works (<https://www.nbarchive.dk/publications/bcw/>)
- [5] https://en.wikipedia.org/wiki/Measurement_problem
- [6] 't Hooft, "The Cellular Automaton Interpretation of Quantum Mechanics" (Springer, 2016), <https://link.springer.com/book/10.1007/978-3-319-41285-6>
- [7] Melinda Baldwin, *Physics Today* <https://pubs.aip.org/physicstoday/online/5262/Q-A-Gerard-t-Hooft-on-the-future-of-quantum>, DOI: <https://doi.org/10.1063/PT.6.4.20170711a>
- [8] A. Yariv, "Quantum Electronics", John Wiley & Sons, Inc., New York, 1989
- [9] Purdue University, ECE 604, Lecture 33, <https://engineering.purdue.edu/wcchew/ece604s19/Lecture%20Notes/Lect33.pdf>
- [10] M. Marte, S. Stenholm, "Paraxial light and atom optics: The optical Schrödinger equation and beyond", *PHYSICAL REVIEW A VOLUME 56, NUMBER 4 OCTOBER 1997*, DOI:<https://doi.org/10.1103/PhysRevA.56.2940>
- [11] L.Schiff, "Quantum Mechanics", McGraw-Hill Inc. third edition 1955
- [12] Li Hua Yu, Chang-Pu Sun, *PHYSICAL REVIEW A VOLUME 49, NUMBER 1 JANUARY 1994*